Weierstraß–Institut
für Angewandte Analysis und Stochastik

im Forschungsverbund Berlin e.V.

Wavelets in numerical analysis and their quantitative properties

Wolfgang Dahmen[1] , Angela Kunoth[2] , Karsten Urban[1]

submitted: 11th March 1997

[1] Institut für Geometrie
und Praktische Mathematik
RWTH Aachen
D – 52056 Aachen
Germany

[2] Weierstraß–Institut
für Angewandte Analysis
und Stochastik
Mohrenstraße 39
D – 10117 Berlin
Germany

Abstract. We discuss various instances where wavelets on the interval serve as building blocks for extending wavelet methods to problems that are neither periodic nor defined on the whole Euclidean space. We then briefly review several properties of such wavelets which are relevant for the previously mentioned applications. Finally, we take a closer look at the quantitative stability properties of wavelets on the interval and indicate ways of improving them.

§1. Introduction

So far wavelet methods unfold their full computational efficiency mainly when applied to problems defined on the whole Euclidean space or on the torus. In this case all the essential algorithmic ingredients are *stationary* with respect to dilation and integer translation. Thus, Fourier techniques not only support the speed of calculations but also the construction, analysis and fine tuning of a rich family of versatile tools. Some of the characteristic properties of wavelets suggest their application, in particular, to the numerical treatment of operator equations. We briefly recall first some of the main driving mechanisms in this context. Then we discuss principal strategies of extending the applicability of wavelet techniques to problems formulated on more general domains. Specifically, we focus on the role of wavelets on the interval as a core ingredient of such developments. After briefly reviewing recent related constructions and results we conclude with a detailed analysis of the quantitative stability properties of such bases on the interval. While on one hand biorthogonal wavelets seem to have several conceptual advantages over orthonormal ones, their quantitative properties reflected e.g. by Riesz constants are expected to be weaker. In fact, our first experiments (see also [29]) revealed that without taking sufficient care, the condition of the generator bases

and the multiscale transformation becomes critically bad for higher degrees of polynomial exactness. Therefore, a central objective of this paper is to develop stabilizing strategies.

Recall that the simplest format of a wavelet basis for $L_2(\mathbb{R}^n)$ can be described as follows. Let $\nabla := \{\lambda = 2^{-j}(\frac{e}{2} + k) : e \in \{0,1\}^n \setminus \{0\}^n,\ j \in \mathbb{Z}, k \in \mathbb{Z}^n\}$ denote the standard *dyadic* grid in scale–space domain, and let

$$\Psi = \{\psi_\lambda : \lambda \in \nabla\},$$

where for some *refinable function* $\varphi \in L_2(\mathbb{R}^n)$

$$\psi_\lambda = 2^{nj/2}\psi_e(2^j \cdot -k), \quad \psi_e(x) = \sum_{k \in \mathbb{Z}^n} a_k^e \varphi(2x - k). \qquad (1.1)$$

It is well known that there exist even compactly supported *scaling functions* φ such that Ψ is a complete orthonormal set in $L_2(\mathbb{R}^n)$ consisting only of compactly supported functions with $\mathrm{diam}\,(\mathrm{supp}\ \psi_\lambda)$ behaving like $2^{-|\lambda|}$ [22], where for $\lambda = 2^{-j}(\frac{e}{2} + k)$ we set $|\lambda| = j$. In this case every $f \in L_2(\mathbb{R}^n)$ has a unique expansion

$$f = \sum_{\lambda \in \nabla}\langle f, \psi_\lambda \rangle_{\mathbf{R}^n}\psi_\lambda, \quad \|\{\langle f, \psi_\lambda\rangle_{\mathbf{R}^n}\}_{\lambda \in \nabla}\|_{\ell_2(\nabla)} = \|f\|_{L_2(\mathbf{R}^n)}, \qquad (1.2)$$

where

$$\langle f, g\rangle_\Omega := \int_\Omega f(x)\overline{g(x)}dx,$$

and for $c = \{c_k\}_{k \in J}$ we denote by $\|c\|_{\ell_2(J)}^2 = \sum_{k \in J}|c_k|^2$ the Euclidean norm of the sequence c.

There are several ways of extending this concept. For instance, instead of employing a *single* generator φ, one could work with a fixed finite collection of generators $\varphi_i,\ i = 1, \ldots, r$, which gives rise to so called *multiwavelets* (see e.g. [2, 23, 31]). One could also relax the requirement of orthonormality. The latter is often rather restrictive, and interferes with *localization*. To describe the various options, it will be very convenient to view expansions of the above type formally as the standard scalar product of a coefficient vector with a (column) vector of basis functions, i.e.,

$$\sum_{\lambda \in \nabla} d_\lambda \psi_\lambda =: \mathbf{d}^T \Psi.$$

Likewise, for any two countable collections $\Theta, \Phi \subset L_2(\Omega)$, we consider the matrix

$$\langle \Theta, \Phi\rangle_\Omega := (\langle \theta, \varphi\rangle_\Omega)_{\theta \in \Theta, \varphi \in \Phi}.$$

Thus, in particular, for $v \in L_2(\Omega)$ the quantities $\langle v, \Phi\rangle_\Omega, \langle \Phi, v\rangle_\Omega$ will always denote row and column vectors, respectively.

The importance of (1.2) for many applications lies in the strong interrelation between the *continuous* world of function spaces with the *discrete* realm of sequences. This is not confined to orthonormal bases. If one is willing to give up on equality in the second relation in (1.2) and is content with both norms being equivalent, it suffices to work with *Riesz bases*. This is known to imply the existence of a *biorthogonal* Riesz basis $\tilde{\Psi}$, i.e.,

$$\langle \Psi, \tilde{\Psi} \rangle_{\mathbf{R}^n} = \mathbf{I}. \tag{1.3}$$

Here the elements in $\tilde{\Psi}$ are defined exactly as in (1.1) with another refinable function $\tilde{\varphi} \in L_2(\mathbb{R}^n)$ satisfying

$$\langle \varphi, \tilde{\varphi}(\cdot - k) \rangle_{\mathbf{R}^n} = \delta_{0,k}, \qquad k \in \mathbb{Z}^n.$$

Even then the interrelation between the continuous and discrete settings usually extends to a whole *scale* of function spaces. In fact, denoting by $H^s(\mathbb{R}^n)$ the *Sobolev space* of all those distributions f such that $(1 + |\cdot|^2)^{s/2} \hat{f} \in L_2(\mathbb{R}^n)$ (where $\hat{f}$ is the Fourier transform of f), it is known that for $\gamma := \sup \{s \in \mathbb{R} : \Psi \subset H^s(\mathbb{R}^n)\}$, $\tilde{\gamma} := \sup \{s \in \mathbb{R} : \tilde{\Psi} \subset H^s(\mathbb{R}^n)\}$

$$\|f\|_{H^s(\mathbf{R}^n)} \sim \|\mathbf{D}^s \langle f, \Psi \rangle_{\mathbf{R}^n}\|_{\ell_2(\nabla)}, \quad s \in (-\tilde{\gamma}, \gamma), \tag{1.4}$$

[22, 30]. Here $\mathbf{D}^s$ is the biinfinite diagonal matrix defined by $(\mathbf{D}^s)_{\lambda,\lambda'} = 2^{s|\lambda|}\delta_{\lambda,\lambda'}$, and $A \sim B$ means that $A \lesssim B$ and $B \lesssim A$ where the latter relation is to express that B can be bounded by a constant times A uniformly in any parameters on which A and B may depend. Norm equivalences of the type (1.4) play a key role in several contexts such as preconditioning, matrix compression (see e.g. [19]) and the design of adaptive strategies for elliptic problems [15].

However, these applications naturally arise in connection with *bounded domains*. The simplest model to which the above machinery extends without much difficulty are periodic problems where $\mathbb{R}^n$ is replaced by the torus $\mathbb{R}^n / \mathbb{Z}^n$. In fact, the index set ∇ now has the form $\nabla = \nabla_+ \cup \nabla_-$, where $\nabla_+ = \{\lambda = 2^{-j_0} k : k \in \mathbb{Z}^n / 2^{j_0} \mathbb{Z}^n\}$ for some $j_0 \in \mathbb{N}$, and $\nabla_- = \{\lambda = 2^{-j}(\frac{e}{2} + k) : e \in \{0,1\}^n \setminus \{0\}^n, k \in \mathbb{Z}^n / 2^j \mathbb{Z}^n, j \geq j_0\}$, and the elements of Ψ are replaced by their *periodized* versions

$$\psi_\lambda = 2^{nj/2} \sum_{m \in \mathbb{Z}^n} \psi_e(2^j(\cdot + m) - k).$$

The Sobolev spaces on the torus can be characterized analogously by the decay properties of the Fourier coefficients. In particular, $H^{-s}(\mathbb{R}^n / \mathbb{Z}^n) = (H^s(\mathbb{R}^n / \mathbb{Z}^n))^*$ is the *dual* of $H^s(\mathbb{R}^n / \mathbb{Z}^n)$. The periodized bases give rise to norm equivalences that are completely analogous to (1.4).

We outline next one important implication of (1.4). Suppose that $\Psi, \tilde{\Psi}$ is a pair of biorthogonal wavelet bases and that the linear operator $\mathcal{A} : H^t(\mathbb{R}^n / \mathbb{Z}^n) \to H^{-t}(\mathbb{R}^n / \mathbb{Z}^n)$ is boundedly invertible, i.e.,

$$\|\mathcal{A}u\|_{H^{-t}(\mathbf{R}^n / \mathbf{Z}^n)} \sim \|u\|_{H^t(\mathbf{R}^n / \mathbf{Z}^n)}.$$

This is known to be the case for a wide range of elliptic pseudo-differential operators. Obviously $u \in H^t(\mathbb{R}^n / \mathbb{Z}^n)$ is the unique solution of the operator equation

$$\mathcal{A}u = f, \quad f \in H^{-t}(\mathbb{R}^n / \mathbb{Z}^n), \tag{1.5}$$

if and only if $\langle \mathcal{A}u, \Psi \rangle_\square = \langle f, \Psi \rangle_\square$, where $\square := [0,1]^n$. Making the ansatz $u = \mathbf{d}^T \Psi$, this gives rise to the (infinite) discrete system

$$\langle \mathcal{A}\Psi, \Psi \rangle_\square^T \mathbf{d} = \langle f, \Psi \rangle_\square^T. \tag{1.6}$$

The matrix $\langle \mathcal{A}\Psi, \Psi \rangle_\square^T$ is the representation of $\mathcal{A}$ in wavelet coordinates. Of course, selecting any finite subset Λ of ∇ and replacing Ψ by $\Psi_\Lambda = \{\psi_\lambda : \lambda \in \Lambda\}$, gives rise to a finite linear system characterizing the *Galerkin approximation*

$$u_\Lambda \in S(\Psi_\Lambda) := \operatorname{span} \Psi_\Lambda,$$

satisfying

$$\langle \mathcal{A}u_\Lambda, v \rangle_\square = \langle f, v \rangle_\square, \quad v \in S(\Psi_\Lambda).$$

Unfortunately, when $t \neq 0$ the matrices $\mathbf{A}_\Lambda := \langle \mathcal{A}\Psi_\Lambda, \Psi_\Lambda \rangle_\square$ grow increasingly *ill-conditioned* when $\#\Lambda$ gets larger. However, as a consequence of (1.4), one can show that when $|t| < \gamma, \tilde{\gamma}$ the operator

$$\mathbf{B} := \mathbf{D}^{-t} \langle \mathcal{A}\Psi, \Psi \rangle_\square^T \mathbf{D}^{-t} \tag{1.7}$$

is boundedly invertible on $\ell_2(\nabla)$, i.e., the corresponding sections $\mathbf{B}_\Lambda$ are uniformly well-conditioned [19]

$$\|\mathbf{B}_\Lambda\| \|\mathbf{B}_\Lambda^{-1}\| = \mathcal{O}(1), \quad \#\Lambda \to \infty, \tag{1.8}$$

where $\|\cdot\|$ denotes the spectral norm. Roughly speaking, the norm equivalence (1.4) allows one to undo the shift in the Sobolev scale caused by the operator $\mathcal{A}$. The continuous problem is thereby transformed into a discrete one which is well-posed with respect to the Euclidean metric. In practical terms this means that, if these matrices were (nearly) sparse, the corresponding linear systems could be efficiently solved by *iterative methods*. The fact that the near sparseness does in fact hold for a wide range of operators, including integral operators, is due to yet another important property of wavelets, namely, their *cancellation* property. For wavelets on $\mathbb{R}^n$ this is conveniently expressed in terms of *vanishing moments*, i.e.,

$$\int_{\mathbb{R}^n} x^\alpha \psi_e(x)\,dx = 0, \quad e \in E_* := \{0,1\}^n \setminus \{0\}^n, \quad |\alpha| < \tilde{d}. \tag{1.9}$$

The order $\tilde{d}$ of vanishing moments of ψ_e is here exactly the order of *polynomial exactness* of the dual generator $\tilde{\varphi}$. This means that any polynomial of order

at most $\bar{d}$ can be represented as a linear combination of the integer translates of $\tilde{\varphi}$ (cf. (3.9) below). It is well–known that for operators of the form

$$\mathcal{A}u = \int K(\cdot, x)u(x)dx,$$

where $K(x, y)$ is smooth except on the diagonal $x = y$, the above cancellation effect causes those entries $\langle \mathcal{A}\psi_{\lambda'}, \psi_\lambda \rangle_\square$ of the matrix $\langle \mathcal{A}\Psi, \Psi \rangle_\square$ to become smaller when either the supports of $\psi_{\lambda'}$ and ψ_λ or their respective scales $|\lambda'|, |\lambda|$ are far apart from each other (see e.g. [16, 19]). This decay is the stronger the higher the order $\bar{d}$ of vanishing moments is. This is an important instance where biorthogonal wavelets offer more flexibility than orthonormal ones. In fact, suppose that the order of exactness of the trial spaces $S(\Psi_\Lambda)$ themselves is d. It turns out that even when $t < 0$, for certain operators $\mathcal{A}$ of the above form, the matrices $\mathbf{B}_\Lambda$ can be replaced by *sparsified* matrices $\mathbf{B}_\Lambda^S$ containing only an order of nonvanishing entries which remains proportional to their size, while the solution of the correspondingly perturbed linear system still exhibits the same asymptotic accuracy as that of the full system, provided that the order $\bar{d}$ of vanishing moments is *strictly larger* than the order d of exactness of the trial spaces [16, 19].

The behavior of the coefficient sequence $\langle f, \tilde{\Psi} \rangle_{\mathbf{R}^n}$ of a function $f = \langle f, \tilde{\Psi} \rangle_{\mathbf{R}^n} \Psi$ expanded in terms of the basis Ψ is determined in a similar way by the local regularity of f. Now the order of vanishing moments of $\tilde{\Psi}$, i.e., the exactness of $\tilde{\Psi}$, determines the decay in $\langle f, \tilde{\Psi} \rangle_{\mathbf{R}^n}$. Thus, when f is smooth except at isolated places, which is the case for the solutions to many elliptic operator equations, one expects that only relatively few of the coefficients in $\langle f, \tilde{\Psi} \rangle_{\mathbf{R}^n}$ are actually needed to represent f accurately. The analysis of a corresponding adaptive algorithm for approximating the solution to an elliptic operator equation in [15] relies in an essential way on both effects, namely, on the norm equivalences (1.4) as well as on the compression effect resulting from cancellation properties like (1.9) for $\bar{d}$ sufficiently large.

Another class of problems where the biorthogonal framework for flexible choices of d and $\bar{d}$ is very useful is the discretization of *saddle point problems*. A typical instance arises in connection with the weak formulation of the Stokes equation. It is well–known that the trial spaces for velocity and pressure have to satisfy a *uniform inf–sup condition* in order to admit an asymptotically stable discretization. It is shown in [17] how to use biorthogonal wavelets to construct such stable pairs for any spatial dimension and any order of exactness. Moreover, this construction is closely related to the construction of compactly supported *divergence free* wavelets [28, 32, 33]. If one wants to approximate the velocity at a higher rate of accuracy than the pressure, it is again necessary to choose the order of exactness of the dual wavelets higher than that of the primal ones.

All the above examples show that wavelets as discretization tools are much more sophisticated than conventional discretizations in that corresponding expansions provide very refined information about the underlying object.

In summary, important driving mechanisms of wavelet based schemes in numerical analysis are norm equivalences like (1.4) and cancellation properties like (1.9). In particular, in many cases it is desirable to have a larger order of vanishing moments than the order of exactness of the primal multiresolution spaces. On the other hand, the realization of these crucial properties (1.4), (1.9) seems to impose significant constraints on the underlying domain.

Several strategies to overcome these limitations are conceivable. One can try to adapt the wavelet basis to the underlying domain. It has been shown in [14] that this is, in principle, possible for rather general Lipschitz domains. However, the precise practical ramifications of this approach are not clear yet. An alternative is to embed a given problem defined on a domain Ω into a problem defined on a simpler domain such as the torus (see e.g. [25]) and treat boundary conditions separately [4, 5, 27]. This may not be suitable in the presence of boundary layers or even impossible when the underlying domain is a closed surface. This latter case is of particular interest for the treatment of boundary integral equations. There is a third possibility which will be addressed in the following section.

§2. Composing Local Wavelet Bases

The starting point is that much of the sophistication of wavelet bases on Euclidean space or on the torus is retained by such bases on cubes. Again let $\square := [0,1]^n$. Many operator equations of practical interest are formulated on domains which can be represented as the essentially disjoint union of parametric images of $\square$, i.e.,

$$\Omega = \bigcup_{i=1}^{N} \kappa_i(\square), \tag{2.1}$$

where the $\kappa_i : \mathbb{R}^n \to \mathbb{R}^{n'}$, $n \leq n'$, are regular parametrizations. Thus, Ω could be a bounded domain in $\mathbb{R}^n$ as well as a closed 2–dimensional surface in $\mathbb{R}^3$. Concerning this latter case one can resort to extensive software developed in the CAGD community. Here the individual mappings κ_i are polynomial or rational transformations usually represented in Bernstein–Bézier form, so that the global smoothness of Ω can be expressed in terms of relations between the control coefficients of adjacent patches. In such a case it is natural to try to induce wavelet bases on the global manifold Ω composed of wavelet bases defined initially only on the individual patches $\Omega_i = \kappa_i(\square)$. The bases on Ω_i, in turn, can be *lifted* from $\square$ as follows. Suppose that $\Psi^\square, \tilde{\Psi}^\square$ is a pair of biorthogonal wavelet bases on $\square$. Due to the regularity of the κ_i, the inner product

$$(f,g)_i := \int_\square f(\kappa_i(x))\overline{g(\kappa_i(x))}\,dx$$

induces a norm which is equivalent to the canonical L_2–norm on Ω_i. Clearly the collections

$$\Psi^i := \Psi^\square \circ \kappa_i^{-1}, \qquad \tilde{\Psi}^i := \tilde{\Psi}^\square \circ \kappa_i^{-1} \tag{2.2}$$

are biorthogonal wavelet bases for the local space $L_2(\Omega_i)$ relative to the inner product $(\cdot, \cdot)_i$. Likewise

$$(\cdot, \cdot) := \sum_{i=1}^{N} (\cdot, \cdot)_i$$

is equivalent in the above sense to $\langle \cdot, \cdot \rangle_\Omega$. Thus, if $\Psi^\square$ is a Riesz basis for $L_2(\square)$ then

$$\Psi^\Omega := \bigcup_{i=1}^{N} \chi_{\kappa_i(\square)} \Psi^i \qquad (2.3)$$

forms a Riesz basis for $L_2(\Omega)$. Of course, the Riesz–bounds (i.e., the constants in (4.1) below) depend on the mappings κ_i, and strong distortions are expected to effect these bounds in a negative way.

However, as pointed out in the previous section, the quality of a wavelet basis for the treatment of operator equations depends on more than just L_2-stability unless the operator has order zero. Of course, for the simple construction (2.3) the cancellation properties of $\Psi^\square$ immediately carry over, [20]. A more subtle question concerns the validity of relations like (1.4) with respect to the global spaces $H^s(\Omega)$. For the definition of such function spaces on manifolds or domains see e.g. [1, 10, 20, 21]. If the basis $\Psi^\square$ gives rise to norm equivalences of the form (1.4) with respect to $\square$, it is not hard to verify that, due to the regularity of the κ_i, the transported bases $\Psi^\square \circ \kappa_i^{-1}$ induce analogous relations for the spaces $H^s(\Omega_i)$ [20]. However, concerning the validity of (1.4) for the global Sobolev space, one problem is that $H^s(\Omega)$ is in general only a closed subspace of the space consisting of those functions on Ω for which

$$\| \cdot \|_s := \left(\sum_{i=1}^{N} \| \cdot \|_{H^s(\Omega_i)}^2 \right)^{1/2} \qquad (2.4)$$

is finite. In fact, both spaces disagree for $s \geq 1/2$. Obviously, the bases on the individual patches have to be properly interrelated in order to give rise to the desired norm equivalences on Ω for a larger range of Sobolev indices s.

In this regard several attempts towards this goal have been made in the literature. A natural strategy is to glue the elements of adjacent local bases Ψ^i across the patch boundaries together [6, 20, 26]. So far this has been done with different degrees of generality in [20, 26] resulting in globally continuous bases. The core ingredients are biorthogonal wavelet bases on $\square$ obtained as tensor products of univariate bases on $[0, 1]$. The same ingredients are used in the work in progress in [6] where the glueing strategy is somewhat different. Although global continuity covers a wide range of problems of practical interest this approach still has some drawbacks. The realization of higher global smoothness along these lines does not seem to be practically feasible. Also duality is not satisfactorily handled for the global space which is a result of the above choice of norms. Finally the glueing seems to adversely affect the cancellation properties near the patch boundaries. Recent results on piecewise polynomial multiwavelets on the interval [23] seem to offer an interesting

alternative, since one only has to worry about glueing the primal basis functions together. However, this ties the number of vanishing moments to the order of exactness of the trial spaces and thus may limit the compression rate. An alternative strategy is based on earlier results by Ciesielski and Figiel [10] concerning unconditional bases for function spaces on smooth manifolds. A key ingredient of this approach is to establish first a topological isomorphism

$$T : H^s(\Omega) \to \prod_{i=1}^N H^s(\Omega_i|B_i) \qquad (2.5)$$

between the global space $H^s(\Omega)$ and the local spaces $H^s(\Omega_i|B_i)$ which are closed subspaces of $H^s(\Omega_i)$ determined by certain homogeneous trace conditions indicated here by B_i. The mapping T has the form

$$Tv = \chi_{\Omega_i} P_i v,$$

where P_i are certain projectors whose image is $H^s(\Omega_i|B_i)$. The range of s (within the limits for which $H^s(\Omega)$ is well–defined) depends on the continuity properties of the projectors P_i. In order to have analogous representations for the duals of these spaces corresponding properties have to hold for the adjoints P_i^* as well. These continuity properties in turn can be completely derived from similar continuity requirements of certain extension operators E_i and their adjoints E_i^* [21]. Thus, the actual realization of T essentially reduces to the construction of such appropriate extensions [10, 21].

The construction of wavelet bases on Ω which satisfy the analog to (1.4) can now be reduced, thanks to the isomorphism T, to the construction of suitable wavelet bases on $\square$ whose lifts through the mappings κ_i obey the boundary conditions imposed by $H^s(\Omega_i|B_i)$. It is shown in [21] how to construct suitable pairs of biorthogonal wavelet bases on $\square$ that satisfy all these requirements and also have the full cancellation properties.

Thus, the common ground for all the above approaches is to have a sufficiently versatile collection of wavelet bases on $\square$. Such wavelets are conveniently constructed via tensor products of wavelets on the interval $[0, 1]$. These, in turn, have been intensely studied in the literature [3, 9, 13, 18]. The above comments indicate that versatility in the present context means good localization of primal and dual bases as well as a possibly flexible choice of the order d of exactness (controlling the accuracy of the discretization scheme), and the order $\tilde{d}$ of vanishing moments (controlling the compression power), which depends on the exactness of the dual multiresolution.

The basic strategy for realizing polynomial exactness in the primal multiresolution spaces is essentially the same in all the above mentioned papers. To ensure the validity of moment conditions throughout the interval $[0, 1]$ requires also the exactness of the dual spaces. This issue has been carefully studied in [18]. Based on this construction the question of incorporating certain (complementary) pairs of boundary conditions needed in connection with the above isomorphism T or for the glueing process mentioned before are studied in [20, 21]. Therefore we focus in the following on the basic construction in [18], and review briefly the main results in the next section.

§3. Biorthogonal Wavelets on the Interval

A convenient starting point for the construction of biorthogonal wavelets on the interval are corresponding multiresolution sequences defined on $\mathbb{R}$. $\theta \in L_2(\mathbb{R})$ is called *refinable* with *mask* $a = \{a_k\}_{k \in \mathbb{Z}}$ if

$$\theta(x) = \sum_{k \in \mathbb{Z}} a_k \theta(2x - k), \quad x \in \mathbb{R} \ a.e. \tag{3.1}$$

We say that two refinable functions θ, $\tilde{\theta}$ form a *dual pair* if

$$\langle \theta, \tilde{\theta}(\cdot - k) \rangle_{\mathbb{R}} = \delta_{0,k}, \quad k \in \mathbb{Z}. \tag{3.2}$$

It is well known that θ and $\tilde{\theta}$ can be normalized so that

$$\int_{\mathbb{R}} \theta(x) dx = \int_{\mathbb{R}} \tilde{\theta}(x) dx = 1. \tag{3.3}$$

Moreover, it will be convenient to write for $g \in L_2(\mathbb{R})$

$$g_{[j,k]} := 2^{j/2} g(2^j \cdot - k), \quad j, k \in \mathbb{Z}.$$

As above let us abbreviate for any collection $C \subset L_2(\Omega)$

$$S(C) = \mathrm{clos}_{L_2}(\mathrm{span}\, C),$$

the L_2-closure of the linear span of C. Thus, defining

$$S_j = S(\{\theta_{[j,k]} : k \in \mathbb{Z}\}), \quad \tilde{S}_j = S(\{\tilde{\theta}_{[j,k]} : k \in \mathbb{Z}\}), \tag{3.4}$$

refinability is known to imply that the spaces S_j and $\tilde{S}_j$ both form a hierarchy of nested spaces whose closure is dense in $L_2(\mathbb{R})$ and whose intersection consists only of 0. $\theta, \tilde{\theta}$ are called the *generators* of the multiresolution sequence $S = \{S_j\}$, $\tilde{S} = \{\tilde{S}_j\}$. It will be convenient to refer to S and $\tilde{S}$ as *primal* and *dual* multiresolution. Moreover, if $\theta, \tilde{\theta}$ have compact support it is easy to see that for $c = \{c_k\}_{k \in \mathbb{Z}} \in \ell_2(\mathbb{Z})$,

$$\Big\| \sum_{k \in \mathbb{Z}} c_k \theta(\cdot - k) \Big\|_{L_2(\mathbb{R})} \sim \|c\|_{\ell_2(\mathbb{Z})} \sim \Big\| \sum_{k \in \mathbb{Z}} c_k \tilde{\theta}(\cdot - k) \Big\|_{L_2(\mathbb{R})} \tag{3.5}$$

which, due to

$$\big\| \theta_{[j,k]} \big\|_{L_2(\mathbb{R})} = \|\theta\|_{L_2(\mathbb{R})}, \tag{3.6}$$

implies the *uniform stability* of the scaled dilates,

$$\Big\| \sum_{k \in \mathbb{Z}} c_k \theta_{[j,k]} \Big\|_{L_2(\mathbb{R})} \sim \|c\|_{\ell_2(\mathbb{Z})}, \tag{3.7}$$

and likewise for $\tilde{\theta}$.

Recall that under certain decay assumptions on the dual pair polynomial, exactness of the spaces S_j determines their approximation power. We say θ is *exact of order* d if all polynomials of degree at most $d-1$ can be written as a linear combination of the integer translates $\theta(\cdot - k)$. In fact, defining

$$\alpha_{\tilde{\theta},r}(y) := \langle (\cdot)^r, \tilde{\theta}(\cdot - y) \rangle_{\mathbb{R}} \tag{3.8}$$

one has then, in view of (3.2), the explicit representation

$$x^r = \sum_{k \in \mathbb{Z}} \alpha_{\tilde{\theta},r}(k)\theta(x-k), \quad x \in \mathbb{R}, \qquad r = 0, \ldots, d-1, \tag{3.9}$$

which will be used frequently later on.

Once θ and $\tilde{\theta}$ are given it is standard to construct corresponding (mother) wavelets whose dilates span complement spaces $W_j, \tilde{W}_j$ satisfying

$$\tilde{W}_j \perp S_j, \quad W_j \perp \tilde{S}_j, \tag{3.10}$$

see [12].

3.1. Multiresolution and Refinement Relations on the Interval

To construct wavelets on the interval one can pursue an analogous strategy and construct first a pair of multiresolution sequences on $[0,1]$. It has long been recognized that it is not sufficient to simply restrict the spaces S_j to $[0,1]$. The fact that only very small portions of some functions contribute to the interval would seriously hurt the stability of the corresponding bases. Also since the supports of θ and $\tilde{\theta}$ generally differ the count would not match. The common strategy employed in all the quoted papers [3, 9, 13, 18] is to retain only those functions $\theta_{[j,k]}, \tilde{\theta}_{[j,k]}$ whose support is fully contained in $[0,1]$ while forming in addition certain modified basis functions near the end points of the interval by taking fixed linear combinations of functions $\theta_{[j,k]}$ near 0 and 1. These linear combinations have to meet two requirements :
  (a) The resulting complete collection of functions consisting of the interior translates and the modified functions near the end points shall still span all polynomials of order d on $[0,1]$.
  (b) The corresponding linear spans shall still be nested.

Suitable boundary functions are simply obtained by truncating the expansion (3.9). In fact, one readily confirms that

$$\sum_{m \in \mathbb{Z}} \alpha_{\tilde{\theta},r}(m)\,\theta_{[j,m]}(x) = 2^{j/2}(2^j x)^r, \qquad r = 0, \ldots, d-1. \tag{3.1.1}$$

The main implications can be formulated as follows [18].

Lemma 1. *Suppose that θ is refinable with mask $\mathbf{a}$ and has compact support*

$$\operatorname{supp}\theta = [\ell_1, \ell_2]. \tag{3.1.2}$$

For

$$\ell \geq -\ell_1 \tag{3.1.3}$$

define

$$\theta^L_{j,\ell-d+r} := \sum_{m=-\ell_2+1}^{\ell-1} \alpha_{\tilde{\theta},r}(m)\,\theta_{[j,m]}\big|_{\mathbf{R}_+}, \quad r = 0,\ldots,d-1. \tag{3.1.4}$$

Then

$$
\begin{aligned}
\theta^L_{j,\ell-d+r} = \ & 2^{-(r+1/2)}\left(\theta^L_{j+1,\ell-d+r} + \sum_{m=\ell}^{2\ell+\ell_1-1} \alpha_{\tilde{\theta},r}(m)\theta_{[j+1,m]}\right) \\
& + \sum_{m=2\ell+\ell_1}^{2\ell+\ell_2-2} \beta_{\tilde{\theta},r}(m)\theta_{[j+1,m]}
\end{aligned}
\tag{3.1.5}
$$

for $r = 0,\ldots,d-1$, where

$$\beta_{\tilde{\theta},r}(m) := 2^{-1/2}\left(\sum_{q=\lceil \frac{m-\ell_2}{2}\rceil}^{\ell-1} \alpha_{\tilde{\theta},r}(q)\,a_{m-2q}\right). \tag{3.1.6}$$

This refinement equation says that a boundary function can always be written as a boundary function on the next higher scale adjusted by scaled translates of the generator on the next scale. The validity of such relations is of course highly plausible because polynomials trivially rescale and the interior translates are refinable. So the point here is only to identify the coefficients in this relation (which appear to be slightly different from those in [3]).

Similarly, one can construct such boundary functions for the right hand side of the interval. However, if the generator θ has certain symmetry properties, the corresponding right end functions $\theta^R_{j,k}$ can actually be obtained also by symmetry considerations. This will be the case for a particular family of dual pairs which will be discussed next.

Let us denote for a sequence of knots $t_i \leq \cdots \leq t_{i+\ell}$ by $[t_i,\ldots,t_{i+\ell}]f$ the ℓ-th order divided difference of $f \in C^\ell(\mathbb{R})$ at $t_i,\ldots,t_{i+\ell}$. Setting $x_+^\ell := (\max\{0,x\})^\ell$, the *cardinal B-spline* $_d\varphi$ of order $d \in \mathbb{N}$ is defined as

$$_d\varphi(x) := d\,[0,1,\ldots,d]\left(\cdot - x - \lfloor\tfrac{d}{2}\rfloor\right)_+^{d-1}. \tag{3.1.7}$$

Thus, φ is *centered* around $\frac{\mu(d)}{2}$, i.e.,

$$_d\varphi(x + \mu(d)) = {}_d\varphi(-x), \qquad x \in \mathbb{R}, \tag{3.1.8}$$

where $\mu(d) := d \bmod 2$, and has support

$$\text{supp } {}_d\varphi = \left[\tfrac{1}{2}(-d + \mu(d)), \tfrac{1}{2}(d + \mu(d))\right] = \left[-\left\lfloor \tfrac{d}{2}\right\rfloor, \left\lceil \tfrac{d}{2}\right\rceil\right] := [\ell_1, \ell_2] \quad (3.1.9)$$

i.e., $d = \ell_2 - \ell_1$ and $\mu(d) = \ell_1 + \ell_2$. Thus, the B–splines of even order are centered around 0 while the ones of odd order are symmetric around $\frac{1}{2}$. The B–spline ${}_d\varphi$ is *refinable* with finitely supported real mask $\mathbf{a} = \{a_k\}_{k=\ell_1}^{\ell_2}$, i.e.,

$$_d\varphi(x) = \sum_{k=\ell_1}^{\ell_2} 2^{1-d} \begin{pmatrix} d \\ k + \lfloor \tfrac{d}{2}\rfloor \end{pmatrix} {}_d\varphi(2x - k) =: \sum_{k=\ell_1}^{\ell_2} a_k\, \varphi(2x - k). \quad (3.1.10)$$

It has been shown in [12] that for each d and any $\tilde{d} \geq d$, $\tilde{d} \in \mathbb{N}$, so that $d + \tilde{d}$ even, there exists a function ${}_{d,\tilde{d}}\tilde{\varphi}$ with the following properties :

(i) ${}_{d,\tilde{d}}\tilde{\varphi}$ has compact support,

$$\text{supp } {}_{d,\tilde{d}}\tilde{\varphi} = [\ell_1 - \tilde{d} + 1, \ell_2 + \tilde{d} - 1] =: [\tilde{\ell}_1, \tilde{\ell}_2]. \quad (3.1.11)$$

(ii) ${}_{d,\tilde{d}}\tilde{\varphi}$ is refinable with finitely supported mask $\tilde{\mathbf{a}}$,

$$_{d,\tilde{d}}\tilde{\varphi}(x) = \sum_{k=\tilde{\ell}_1}^{\tilde{\ell}_2} \tilde{a}_k\, {}_{d,\tilde{d}}\tilde{\varphi}(2x - k). \quad (3.1.12)$$

(iii) ${}_{d,\tilde{d}}\tilde{\varphi}$ has the same symmetry properties as ${}_d\varphi$, i.e.,

$$_{d,\tilde{d}}\tilde{\varphi}(x + \mu(d)) = {}_{d,\tilde{d}}\tilde{\varphi}(-x), \quad x \in \mathbb{R}. \quad (3.1.13)$$

(iv) The functions ${}_d\varphi$ and ${}_{d,\tilde{d}}\tilde{\varphi}$ form a *dual pair*, i.e.,

$$\langle {}_d\varphi, {}_{d,\tilde{d}}\tilde{\varphi}(\cdot - k)\rangle_\mathbb{R} = \delta_{0,k}, \quad k \in \mathbb{Z}. \quad (3.1.14)$$

(v) ${}_{d,\tilde{d}}\tilde{\varphi}$ is exact of order $\tilde{d}$, i.e., all polynomials of degree less than $\tilde{d}$ can be represented as linear combinations of the translates ${}_{d,\tilde{d}}\tilde{\varphi}(\cdot - k), k \in \mathbb{Z}$.

(vi) The regularity of ${}_{d,\tilde{d}}\tilde{\varphi}$ is proportional to $\tilde{d}$.

In the following $d, \tilde{d}$ will be arbitrary as above but fixed so that we suppress them as indices and write briefly $\varphi, \tilde{\varphi}$.

In contrast to earlier papers the above boundary modifications have been applied in [18] to both the primal as well as the dual multiresolution for the following reasons :

- This ensures that the primal wavelets have $\tilde{d}$ vanishing moments on all of $[0, 1]$.
- In connection with the discretization of saddle point problems both multiresolution sequences represent physical quantities (e.g. velocity and pressure) that have to be resolved accurately.

- The validity of norm equivalences of the type (1.4) on $[0,1]$ for the negative range of Sobolev indices depends on the exactness of the dual multiresolution (see [18]).

To this end, we wish to determine pairs of bases Φ_j, $\tilde{\Phi}_j$ of the following format

$$\Phi_j = \Phi_j^L \cup \Phi_j^I \cup \Phi_j^R, \quad \tilde{\Phi}_j = \tilde{\Phi}_j^L \cup \tilde{\Phi}_j^I \cup \tilde{\Phi}_j^R, \qquad (3.1.15)$$

where the Φ_j^I, $\tilde{\Phi}_j^I$ consist of interior translates $\varphi_{[j,k]}, k \in \Delta_j^I$, $\tilde{\varphi}_{[j,k]}, k \in \tilde{\Delta}_j^I$, while the Φ_j^X, $\tilde{\Phi}_j^X$ contain the boundary functions $\varphi_{j,k}^X, k \in \Delta_j^X$, $\tilde{\varphi}_{j,k}^X, k \in \tilde{\Delta}_j^X$, $X \in \{L, R\}$. The $\varphi_{j,k}^L$, $\tilde{\varphi}_{j,k}^L$ are defined according to the recipe (3.1.4) and the right end counterparts are defined in a completely analogous fashion where the monomials x^r are replaced by $(1 - x)^r$. Since by (3.1.11) the support of $\tilde{\varphi}$ is always larger than that of φ, i.e., $\tilde{\ell}_2 \geq \ell_2$, $-\tilde{\ell}_1 \geq -\ell_1$ (even if $\tilde{d} < d$), one has to determine first the number of translates involved in the boundary modifications on the dual side. Thus, we fix some integer $\tilde{\ell}$ satisfying

$$\tilde{\ell} \geq \tilde{\ell}_2, \qquad (3.1.16)$$

so that the indices

$$\tilde{\Delta}_j^I := \{\tilde{\ell}, \ldots, 2^j - \tilde{\ell} - \mu(d)\} \qquad (3.1.17)$$

correspond to translates $\tilde{\varphi}_{[j,m]}$ whose supports are contained in $[0,1]$. In order to ensure that $\tilde{\Delta}_j^I$ is not empty, we will always assume that

$$j \geq j_0 := \left\lceil \log_2(\tilde{\ell} + \tilde{\ell}_2 - 1) + 1 \right\rceil. \qquad (3.1.18)$$

By (3.1.4), the corresponding boundary index sets are

$$\tilde{\Delta}_j^L := \{\tilde{\ell} - \tilde{d}, \ldots, \tilde{\ell} - 1\}, \quad \tilde{\Delta}_j^R := \{2^j - \tilde{\ell} + 1 - \mu(d), \ldots, 2^j - \tilde{\ell} + \tilde{d} - \mu(d)\}. \qquad (3.1.19)$$

The shift by $\mu(d)$ in $\tilde{\Delta}_j^R$ and $\tilde{\Delta}_j^I$ has been included in order to make best possible use of symmetry later.

Given $\tilde{\ell}$, the corresponding parameter ℓ for the primal bases will always be chosen as

$$\ell := \tilde{\ell} - (\tilde{d} - d), \qquad (3.1.20)$$

in order to ensure that

$$\tilde{\Delta}_j := \tilde{\Delta}_j^L \cup \tilde{\Delta}_j^I \cup \tilde{\Delta}_j^R = \Delta_j = \Delta_j^L \cup \Delta_j^I \cup \Delta_j^R. \qquad (3.1.21)$$

Note that the larger ℓ (or equivalently $\tilde{\ell}$) is, the larger is the interval near zero where the boundary function $\varphi_{j,\ell-d+r}^L$ coincides with the polynomial $2^{j/2}(2^j x)^r$, a fact that will be of some importance later.

As mentioned before one can now exploit symmetry.

Remark 2. *One has for $x \in [0,1]$*

$$\varphi^R_{j,2^j-\ell+d-\mu(d)-r}(1-x) = \varphi^L_{j,\ell-d+r}(x), \quad r = 0,\ldots,d-1,$$

$$\tilde{\varphi}^R_{j,2^j-\tilde{\ell}+\tilde{d}-\mu(d)-r}(1-x) = \tilde{\varphi}^L_{j,\tilde{\ell}-\tilde{d}+r}(x), \quad r = 0,\ldots,\tilde{d}-1,$$

(3.1.22)

and

$$\theta_{[j,m]}(x) = \theta_{[j,2^j-m-\mu(d)]}(1-x), \quad \theta = \varphi, \tilde{\varphi}, \quad m \in \Delta^I_j. \quad (3.1.23)$$

Moreover, defining

$$\varphi_{j,k} := \begin{cases} \varphi^X_{j,k}, & k \in \Delta^X_j, X \in \{L,R\}, \\ \varphi_{[j,k]}, & k \in \Delta^I_j, \end{cases}$$

let

$$\Phi_j := \{\varphi_{j,k} : k \in \Delta_j\} \quad (3.1.24)$$

and similarly

$$\tilde{\Phi}'_j := \{\tilde{\varphi}^L_{j,k} : k \in \tilde{\Delta}^L_j\} \cup \{\tilde{\varphi}_{[j,k]} : k \in \tilde{\Delta}^I_j\} \cup \{\tilde{\varphi}^R_{j,k} : k \in \tilde{\Delta}^R_j\}. \quad (3.1.25)$$

Finally, define

$$S_j := S(\Phi_j), \quad \tilde{S}_j := S(\tilde{\Phi}'_j). \quad (3.1.26)$$

One can now show that these spaces have the desired properties [18].

Proposition 3.
(i) The spaces S_j and $\tilde{S}_j$ are nested, i.e.,

$$S_j \subset S_{j+1}, \quad \tilde{S}_j \subset \tilde{S}_{j+1}, \quad j \geq j_0. \quad (3.1.27)$$

(ii) The spaces S_j, $\tilde{S}_j$ are exact of order d, $\tilde{d}$, respectively, i.e.,

$$\Pi_d([0,1]) \subset S_j, \quad \Pi_{\tilde{d}}([0,1]) \subset \tilde{S}_j, \quad j \geq j_0. \quad (3.1.28)$$

The nestedness of the spaces S_j, $\tilde{S}_j$ is equivalent to the validity of *refinement equations*

$$\varphi_{j,k} = \sum_{l \in \Delta_{j+1}} m^j_{l,k} \varphi_{j+1,l}, \quad k \in \Delta_j.$$

Due to the boundary modifications, the masks in these relations are no longer shift- and scale–invariant. Adhering to the matrix notation employed previously, it will be extremely convenient to rewrite this as

$$\Phi^T_j = \Phi^T_{j+1} \mathbf{M}_{j,0}, \quad (3.1.29)$$

where $M_{j,0}$ is a $(\#\Delta_{j+1}) \times (\#\Delta_j)$–matrix. The format of the refinement matrix $M_{j,0}$ can be illustrated by

$$
M_{j,0} :=
\begin{array}{|c|}
\hline
M_L \quad\quad\quad\quad\quad 0 \\
\quad A_j \\
0 \quad\quad\quad\quad M_R \\
\hline
\end{array}
\tag{3.1.30}
$$

where M_L, M_R are $(d + \ell + \ell_2 - 1) \times d$ blocks representing the refinement relations for the functions in Φ_j^L, Φ_j^R, respectively. By symmetry one has

$$
M_R = M_L^{\updownarrow},
\tag{3.1.31}
$$

where $\updownarrow$ means that the order of rows and columns is reversed. The entries of the blocks M_X can therefore be read off from Lemma 1 (see [18] for more details). The M_X are *independent* of j. The columns in the interior block A_j are the stationary refinement masks from (3.1.10). Their dependence on j lies only in the size of A_j. Accordingly, $M_{j,0}$ can be set up for each $j \geq j_0$ by only knowing M_L and a from (3.1.10). Thus, although one has to give up on complete shift–invariance much of the efficiency of the classical framework can be retained for the interval. Analogous relations hold of course for $\tilde{\Phi}_j'$ with a similar matrix $\tilde{M}_{j,0}'$.

3.2. Biorthogonalization

One important point has yet to be addressed. While the interior functions in the collections $\Phi_j, \tilde{\Phi}_j'$ inherit biorthogonality this is generally no longer true for the boundary modifications. To restore biorthogonality, one has to perform a suitable change of bases near the boundaries. Specifically, one has to determine matrices $C_j, \tilde{C}_j$ such that

$$
\Phi_j^{\mathrm{new}} = C_j \Phi_j, \quad \tilde{\Phi}_j^{\mathrm{new}} = \tilde{C}_j \tilde{\Phi}_j'
\tag{3.2.1}
$$

satisfy

$$
\langle \Phi_j^{\mathrm{new}}, \tilde{\Phi}_j^{\mathrm{new}} \rangle_{[0,1]} = I.
\tag{3.2.2}
$$

Due to the biorthogonality of the interior functions and the symmetry properties the matrices $C_j, \tilde{C}_j$ have the form

$$
C_j = \begin{pmatrix} C_L & 0 & 0 \\ 0 & I & 0 \\ 0 & 0 & C_L^{\updownarrow} \end{pmatrix}, \quad
\tilde{C}_j = \begin{pmatrix} \tilde{C}_L & 0 & 0 \\ 0 & I & 0 \\ 0 & 0 & \tilde{C}_L^{\updownarrow} \end{pmatrix},
\tag{3.2.3}
$$

where the $C_L, \tilde{C}_L$ are $\bar{d} \times \bar{d}$ matrices independent of j. Since

$$\langle \Phi_j^{\text{new}}, \tilde{\Phi}_j^{\text{new}} \rangle_{[0,1]} = C_j \langle \Phi_j, \tilde{\Phi}_j' \rangle_{[0,1]} \tilde{C}_j^T,$$

biorthogonalization is actually possible if and only if

$$\det \langle \Phi_j, \tilde{\Phi}_j' \rangle_{[0,1]} \neq 0. \tag{3.2.4}$$

In fact, setting

$$\Gamma_j := \langle \Phi_j, \tilde{\Phi}_j' \rangle_{[0,1]},$$

the matrices $C_j, \tilde{C}_j$ have to satisfy

$$C_j \Gamma_j \tilde{C}_j^T = I. \tag{3.2.5}$$

Since $\#\Delta_j^L \leq \#\tilde{\Delta}_j^L$ we will denote in the sequel by Φ_j^X the set of cardinality $\bar{d}$ obtained by adding to the functions $\varphi_{j,k}^X, k \in \Delta_j^X$, the approriate number of $\bar{d} - d$ additional interior functions. Then by (3.2.3), the nonsingularity of Γ_j is equivalent to the nonsingularity of

$$\Gamma_L := \langle \Phi_j^L, \tilde{\Phi}_j^L \rangle_{[0,1]}, \tag{3.2.6}$$

which does not seem to be clear beforehand. The following result has been proven in [18].

Theorem 4. *The matrix Γ_L is nonsingular for every admissible choice of $d, \bar{d}$.*

Thus, biorthogonalization is indeed possible. In [18] we have chosen $C_j = I$ which results in

$$\tilde{C}_L = \Gamma_L^{-T}. \tag{3.2.7}$$

Of course, the refinement relations change under such a change of bases. We will several times make use of the following simple observation [18].

Remark 5. *If $\Theta_j^T = \Theta_{j+1}^T M_{j,0}$ and $\Theta_j^{\text{new}} = C_j \Theta_j$ then*

$$(\Theta_j^{\text{new}})^T = (\Theta_{j+1}^{\text{new}})^T M_{j,0}^{\text{new}}, \tag{3.2.8}$$

where

$$M_{j,0}^{\text{new}} = C_{j+1}^{-T} M_{j,0} C_j^T. \tag{3.2.9}$$

The *standard biorthogonal pair* $\Phi_j, \tilde{\Phi}_j$ considered in [18] is given by Φ_j defined in (3.1.24) and

$$\tilde{\Phi}_j = \Gamma_j^{-T} \tilde{\Phi}_j'. \tag{3.2.10}$$

By (3.2.9), the corresponding refinement matrix in

$$\tilde{\Phi}_j^T = \tilde{\Phi}_{j+1}^T \tilde{M}_{j,0} \tag{3.2.11}$$

is, on account of (3.2.5) with $C_j = I$, given by

$$\tilde{M}_{j,0} = \Gamma_{j+1} \tilde{M}_{j,0}' \Gamma_j^{-1}, \tag{3.2.12}$$

where $\tilde{M}_{j,0}'$ is the refinement matrix for $\tilde{\Phi}_j'$ derived from Lemma 1 (see [18] for more details). The nonzero pattern of a typical pair of refinement matrices for $j = j_0 = 6$ and $d = 4, \bar{d} = 8$ is illustrated in Figure 1.
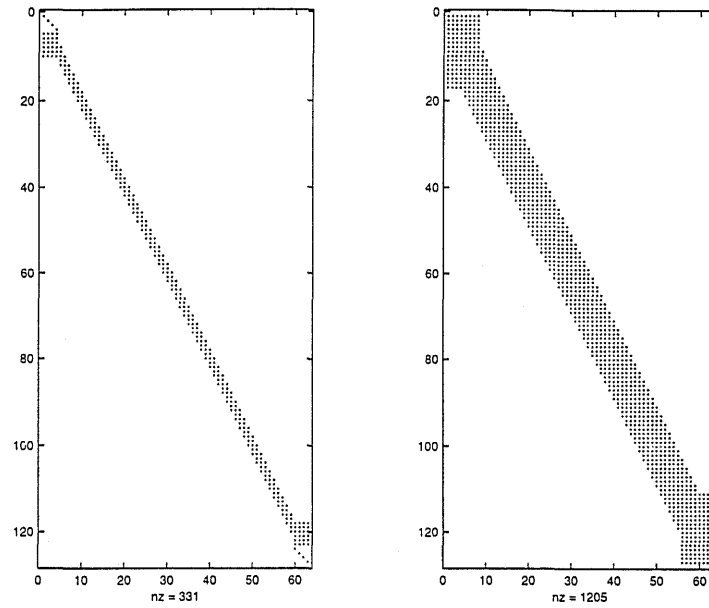
Fig. 1. Nonzero pattern of the matrices $M_{6,0}, \tilde{M}_{6,0}$ for $d = 4$, $\tilde{d} = 8$.

3.3. Biorthogonal Wavelets

Given the above standard pairs Φ_j, $\tilde{\Phi}_j = \Gamma_j^{-T}\tilde{\Phi}'_j$ of biorthogonal bases for the spaces $S_j, \tilde{S}_j$, the next step is to construct corresponding wavelet bases. In [18] a systematic construction of collections

$$\Psi_j^T = \Phi_{j+1}^T M_{j,1}, \quad \tilde{\Psi}_j^T = \tilde{\Phi}_{j+1}^T \tilde{M}_{j,1} \tag{3.3.1}$$

with the following properties is presented:

(i) The matrices $M_j := (M_{j,0}, M_{j,1})$, $\tilde{M}_j := (\tilde{M}_{j,0}, \tilde{M}_{j,1})$ satisfy

$$M_j \tilde{M}_j^T = I. \tag{3.3.2}$$

(ii) The matrices $M_j, \tilde{M}_j$ are uniformly sparse, i.e., the number of nonzero entries in rows and columns remains uniformly bounded in j. Thus, the quasi–stationary character of the refinement matrices is inherited.

(iii) The collections $\Psi_j, \tilde{\Psi}_j$ span complements of $S_j, \tilde{S}_j$ in $S_{j+1}, \tilde{S}_{j+1}$, respectively, and

$$\langle \Psi_j, \tilde{\Phi}_j \rangle_{[0,1]} = \langle \tilde{\Psi}_j, \Phi_j \rangle_{[0,1]} = 0, \quad \langle \Psi_j, \tilde{\Psi}_j \rangle_{[0,1]} = I. \tag{3.3.3}$$

(iv) As a consequence the collections

$$\Psi := \Phi_{j_0} \cup \bigcup_{j=j_0}^{\infty} \Psi_j, \quad \tilde{\Psi} := \tilde{\Phi}_{j_0} \cup \bigcup_{j=j_0}^{\infty} \tilde{\Psi}_j \tag{3.3.4}$$

are biorthogonal,

$$\langle \Psi, \tilde{\Psi} \rangle_{[0,1]} = \mathbf{I}, \tag{3.3.5}$$

and satisfy the norm equivalences

$$\|f\|_{H^s([0,1])} \sim \|\mathbf{D}^s \langle f, \tilde{\Psi} \rangle_{[0,1]}\|_{\ell_2} \tag{3.3.6}$$

for $s \in (-\tilde{\gamma}, d + 1/2)$, where $\tilde{\gamma} := \sup\{s : \tilde{\varphi} \in H^s(\mathbb{R})\}$ ($\tilde{\gamma}$ grows linearly with $\tilde{d}$), and $H^s([0,1])$ is to be understood as the dual of $H^{-s}([0,1])$ when $s < 0$.

(v) Any $\psi \in \Psi \setminus \Phi_{j_0}$ has $\tilde{d}$ vanishing moments, i.e.,

$$\int_0^1 x^r \psi(x) dx = 0, \quad r = 0, \dots, \tilde{d} - 1. \tag{3.3.7}$$

We will need later some information about the construction of the matrices $\mathbf{M}_{j,1}, \tilde{\mathbf{M}}_{j,1}$ in (3.3.1):

- Following [18], the first step is to determine a matrix $\check{\mathbf{M}}_{j,1}$ such that $\check{\mathbf{M}}_j := (\mathbf{M}_{j,0}, \check{\mathbf{M}}_{j,1})$ is invertible, and to identify its inverse

$$\check{\mathbf{M}}_j^{-1} = \begin{pmatrix} \check{\mathbf{G}}_{j,0} \\ \check{\mathbf{G}}_{j,1} \end{pmatrix} =: \check{\mathbf{G}}_j.$$

  Such an $\check{\mathbf{M}}_{j,1}$ is called a *stable completion*. Using results about factorizations of spline collocation matrices, such stable completions were constructed in [18] for any admissible $d, \tilde{d}$ as above in such a way that the matrices $\check{\mathbf{M}}_j$ and their inverses $\check{\mathbf{G}}_j$ are both sparse. This ensures that corresponding multiscale decomposition and reconstruction schemes are efficient.

- Given a biorthogonal pair $\Phi_j, \tilde{\Phi}_j$, e.g. the one given by (3.1.24) and (3.2.10) with refinement matrices $\mathbf{M}_{j,0}, \tilde{\mathbf{M}}_{j,0}$, the stable completions required in (3.3.1) are given by

$$\begin{aligned} \mathbf{M}_{j,1} &= (\mathbf{I} - \mathbf{M}_{j,0}\tilde{\mathbf{M}}_{j,0}^T)\check{\mathbf{M}}_{j,1}\mathbf{K}_j, \\ \tilde{\mathbf{M}}_{j,1} &= \check{\mathbf{G}}_{j,1}^T\mathbf{K}_j^{-1}, \end{aligned} \tag{3.3.8}$$

where $\mathbf{K}_j$ is *any* invertible matrix [7]. In the following we will mainly use $\mathbf{K}_j = \mathbf{I}$ (for corresponding concrete examples see [18]).

The nonzero pattern of a pair of stable completions satisfying (3.3.8) for $j = j_0 = 6$ and $d = 4, \tilde{d} = 8$ which corresponds to the pair in Figure 1 is illustrated in Figure 2.

§4. Quantitative Stability Properties

According to the above results, one can, in principle, construct wavelet bases on $[0,1]$ sharing the desired properties listed before. Likewise this extends to $\square$ and hence to more general domains via the techniques outlined in Section 2.

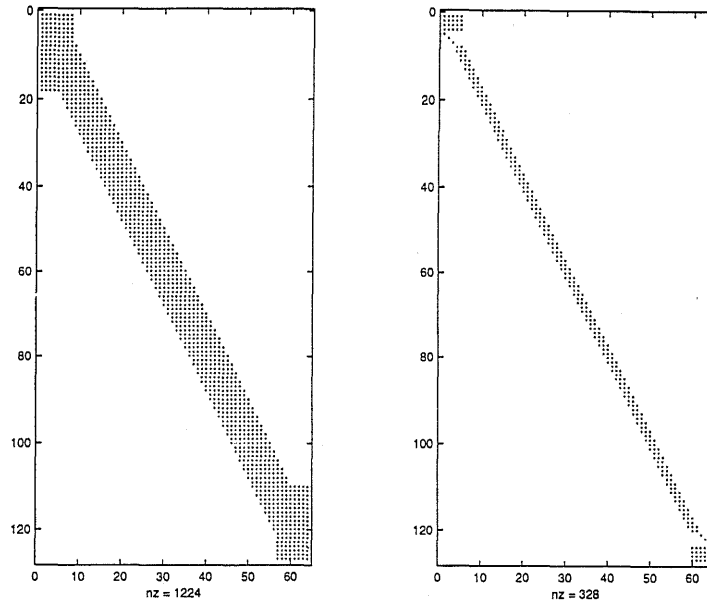**Fig. 2.** Nonzero pattern of the matrices $M_{6,1}, \tilde{M}_{6,1}$ for $d = 4, \tilde{d} = 8$.

Although theory assures that biorthogonalization is always possible, the actual practical value of such tools will ultimately depend on their quantitative properties. The first examples shown in [18] of the above wavelet bases confirmed experiences made earlier with similar constructions. Precisely, recall that whenever Θ is a Riesz basis of the closure of its span, one has

$$c\|\boldsymbol{c}\|_{\ell_2} \leq \|\boldsymbol{c}^T \Theta\|_{L_2} \leq C\|\boldsymbol{c}\|_{\ell_2}, \tag{4.1}$$

and that the positive constants c_1^Θ, c_2^Θ are called the *Riesz bounds* of the basis Θ if

$$\begin{aligned} c_1^\Theta &= \sup\{c : c \text{ satisfies } (4.1)\}, \\ c_2^\Theta &= \inf\{C : C \text{ satisfies } (4.1)\}. \end{aligned}$$

Moreover, it is known that

$$c_1^\Theta = \sqrt{\lambda_{\min}(\langle\Theta,\Theta\rangle)}, \quad c_2^\Theta = \sqrt{\lambda_{\max}(\langle\Theta,\Theta\rangle)}, \tag{4.2}$$

where $\lambda_{\min}(\langle\Theta,\Theta\rangle), \lambda_{\max}(\langle\Theta,\Theta\rangle)$ denote the smallest and largest eigenvalue of the Gramian matrix $\langle\Theta,\Theta\rangle$. By *poorly conditioned* we mean that the quotient c_2^Θ/c_1^Θ called the *condition* of the basis Θ is large. Of course, one expects that a poor condition of the bases adversely effects the multiscale decomposition of signals. Also when the boundary functions behave very irregularly it is not clear how to associate given discrete data with an expansion with respect to the single scale basis Φ_j, say. Moreover, the quantitative approximation properties may suffer as it is indicated by the following considerations. Suppose that $\Phi_j, \tilde{\Phi}_j$ forms a pair of biorthogonal generator bases. Assume

that the elements in Φ_j are normalized so that, in particular, the boundary functions all have L_2-norm one. Since

$$1 = \langle \varphi_{j,k}, \tilde{\varphi}_{j,k} \rangle_{[0,1]} \leq \|\varphi_{j,k}\|_{L_2([0,1])} \|\tilde{\varphi}_{j,k}\|_{L_2([0,1])} = \|\tilde{\varphi}_{j,k}\|_{L_2([0,1])},$$

the norms of the dual functions are always larger than or equal to one. Now consider the approximation behavior of the projector $Q_j f := \langle f, \tilde{\Phi}_j \rangle_{[0,1]} \Phi_j$ at a point x near zero. Recalling that by assumption Q_j reproduces any polynomial p of degree at most $d - 1$, one obtains

$$\|f - Q_j f\|_{L_2([0,2^{-j}])} \leq \|f - p\|_{L_2([0,2^{-j}])} + \sum_{k \in \Delta_j} |\langle f - p, \tilde{\varphi}_{j,k} \rangle_{[0,1]}| \|\varphi_{j,k}\|_{L_2([0,2^{-j}])}.$$

The first summand represents the error of best local L_2-approximation of f by polynomials. The sum on the right hand side is of course finite since only finitely many of the basis functions overlap $[0, 2^{-j}]$. By assumption, the factors $\|\varphi_{j,k}\|_{L_2([0,2^{-j}])}$ are bounded by one, while the weights $|\langle f - p, \tilde{\varphi}_{j,k} \rangle_{[0,1]}|$ can by Schwartz' inequality again be estimated by $\|\tilde{\varphi}_{j,k}\|_{L_2([0,1])}$ times the best local polynomial approximation of f. This local polynomial approximation determines, of course, the asymptotic rate while the factors $\|\tilde{\varphi}_{j,k}\|_{L_2([0,1])}$ apparently influence the constants.

This has motivated further investigations of the quantitative properties of the adapted bases reported below. In the light of the above comments we are, in particular, interested in the following quantities. Let $\mathbf{R}_j := \langle \Phi_j, \Phi_j \rangle_{[0,1]}$ and $\tilde{\mathbf{R}}_j := \langle \tilde{\Phi}_j, \tilde{\Phi}_j \rangle_{[0,1]}$ denote the Gramian matrix of Φ_j and $\tilde{\Phi}_j$, respectively. Accordingly,

$$c_1 := \sqrt{\lambda_{\min}(\mathbf{R}_j)}, \qquad c_2 := \sqrt{\lambda_{\max}(\mathbf{R}_j)}, \tag{4.3}$$

and

$$\tilde{c}_1 := \sqrt{\lambda_{\min}(\tilde{\mathbf{R}}_j)}, \qquad \tilde{c}_2 := \sqrt{\lambda_{\max}(\tilde{\mathbf{R}}_j)}, \tag{4.4}$$

are the Riesz bounds of the bases Φ_j, $\tilde{\Phi}_j$, respectively. The bases Φ_j, $\tilde{\Phi}_j$ are given by (3.1.24) and (3.2.10). Similarly, we set $\mathbf{W}_j := \langle \Psi_j, \Psi_j \rangle_{[0,1]}$ and

$$d_1 := \sqrt{\lambda_{\min}(\mathbf{W}_j)}, \qquad d_2 := \sqrt{\lambda_{\max}(\mathbf{W}_j)}, \tag{4.5}$$

for the wavelet basis Ψ_j defined by (3.3.1) and (3.3.8). The matrices $\tilde{\mathbf{W}}_j$ and the Riesz bounds $\tilde{d}_1, \tilde{d}_2$ are defined in complete analogy when Ψ_j is replaced by $\tilde{\Psi}_j$.

Recall from (3.2.10) that the biorthogonalization in [18] required inversion of the matrices Γ_j and hence, in view of (3.2.3), of Γ_L defined in (3.2.6). As for the accurate and reliable computation of the corresponding refinement matrices, one therefore has to take the condition number of Γ_L into account. Recall also that Γ_L depends on the parameters $d, \tilde{d}, \tilde{\ell}$ determining the order of polynomial exactness of the primal and dual multiresolution, respectively, and

the range near the end points of the interval where the boundary functions agree with polynomials. Recall also that the decomposition and reconstruction algorithms associated with the wavelet bases consist of applying $\mathbf{M}_j$ and $(\mathbf{M}_j)^{-1}$. Therefore, we monitor also their condition numbers.

Thus, a natural starting point is to determine first for the above *standard* construction the spectral condition numbers $\mathrm{cond}(\mathbf{\Gamma}_L)$, $\mathrm{cond}(\mathbf{R}_j)$, $\mathrm{cond}(\tilde{\mathbf{R}}_j)$, $\mathrm{cond}(\mathbf{W}_j)$, $\mathrm{cond}(\tilde{\mathbf{W}}_j)$, the corresponding Riesz bounds c_i, $\tilde{c}_i$, d_i, $\tilde{d}_i$, $i = 1, 2$, $\mathrm{cond}(\mathbf{M}_j)$ and the quantities

$$\varrho := \max_{k \in \Delta_j} \left(\|\tilde{\varphi}_{j,k}\|_{L_2([0,1])} \|\varphi_{j,k}\|_{L_2([0,1])} \right),$$

which are in fact independent of j. To this end, one should note first that all our experiments confirm the expected fact that the Riesz bounds only depend very weakly on j and gradually settle when j grows. Since the dependence of the bases Φ_j, $\tilde{\Phi}_j$ on j lies only in the growth of the interior stationary portions Φ_j^I, $\tilde{\Phi}_j^I$, we conclude that the quantities of interest are mainly influenced by the boundary portions of the bases which are up to scaling also independent of j. Therefore all subsequent calculations will refer to the minimal level $j = j_0$ in each case and $\bar{\ell} = \bar{\ell}_2 = \lceil \frac{d}{2} \rceil + \tilde{d} - 1$.

Let us first look at the first part of Tables 1–3 where the data labeled 'No Transform' corresponds to the original construction in [18]. This data reveals the following facts:

- The condition numbers of $\mathbf{\Gamma}_L$ grow rapidly when d or $\tilde{d}$ becomes larger. A sufficiently accurate calculation of the corresponding refinement matrices therefore requires some care and initially did cause some trouble.
- The condition of the wavelet bases Ψ_j and their duals $\tilde{\Psi}_j$ stay rather moderate for a wide range of $d, \tilde{d}$.
- This is also true for the generator bases Φ_j, $\tilde{\Phi}_j$ for $d = 2$ and any $\tilde{d}$ within the range of our experiments. This is not completely obvious beforehand since the parameter $\bar{\ell}$ (and hence ℓ, see (3.1.16), (3.1.20)) depends on $\tilde{d}$ and thus changes also Φ_j. However, when d grows the condition of Φ_j *and* $\tilde{\Phi}_j$ also increases rapidly again almost independently of $\tilde{d} \geq d$. In fact, already for $d = 4$ the condition of Φ_j, $\tilde{\Phi}_j$ attains a critical size which may severely interfere with the objectives of a corresponding high order scheme. As for the Φ_j, this is, of course, in agreement with the known results about the condition of B–spline bases (see e.g. [8]).
- Like for the Riesz bounds, the parameter ϱ grows rather moderately but attains for $d = 4$ a size where the approximation property near the boundaries may suffer critically. The condition of $\mathbf{M}_j$ also grows rapidly with d almost independently of $\tilde{d} \geq d$.

Now our main concerns will be to improve on the condition of the *standard* generator bases Φ_j, $\tilde{\Phi}_j$, the quantity ϱ and the condition of $\mathbf{\Gamma}_L$. Of course, then the question arises whether corresponding changes also affect the wavelet bases. It turns out that this is actually not the case which will be proved next.

		$d=2$	$\tilde{d}=2$	$\tilde{d}=4$	$\tilde{d}=6$	$\tilde{d}=8$
N	cond(Γ_L)	1.6774e + 01	7.2772e + 02	1.8741e + 05	1.1515e + 08
O	c_2/c_1	4.4422e + 00	4.4413e + 00	4.4413e + 00	4.4413e + 00
	c_1	3.1358e − 01	3.1364e − 01	3.1364e − 01	3.1364e − 01
	c_2	1.3930e + 00	1.3930e + 00	1.3930e + 00	1.3930e + 00
T	$\tilde{c}_2/\tilde{c}_1$	5.0473e + 00	4.6054e + 00	4.8294e + 00	5.3946e + 00
R	$\tilde{c}_1$	7.2816e − 01	7.2099e − 01	7.2356e − 01	7.2283e − 01
A	$\tilde{c}_2$	3.6753e + 00	3.3205e + 00	3.4944e + 00	3.8994e + 00
N	d_2/d_1	3.6122e + 00	3.7006e + 00	3.2977e + 00	2.7335e + 00
S	d_1	2.2285e − 01	2.1869e − 01	2.4700e − 01	3.0076e − 01
F	d_2	8.0497e − 01	8.0928e − 01	8.1452e − 01	8.2212e − 01
O	$\tilde{d}_2/\tilde{d}_1$	3.8469e + 00	3.9731e + 00	4.3317e + 00	4.8178e + 00
R	$\tilde{d}_1$	1.4348e + 00	1.2441e + 00	1.2287e + 00	1.2320e + 00
M	$\tilde{d}_2$	5.5196e + 00	4.9429e + 00	5.3225e + 00	5.9353e + 00
	cond(M_j)	5.3641e + 00	4.7432e + 00	4.4225e + 00	4.4280e + 00
	ϱ	2.5454e + 00	2.2853e + 00	2.4038e + 00	2.5803e + 00
	c_2^{new}/c_1^{new}	1.6673e + 00	1.1350e + 01	2.2554e + 02	6.8118e + 03
	c_1^{new}	5.9548e − 01	1.4688e − 01	1.3852e − 02	8.5578e − 04
S	c_2^{new}	9.9282e − 01	1.6672e + 00	3.1242e + 00	5.8294e + 00
V	$\tilde{c}_2^{new}/\tilde{c}_1^{new}$	1.8891e + 00	1.0796e + 01	1.8861e + 02	4.2374e + 03
D	$\tilde{c}_1^{new}$	1.0075e + 00	6.3455e − 01	3.8305e − 01	2.7620e − 01
	$\tilde{c}_2^{new}$	1.9032e + 00	6.8504e + 00	7.2246e + 01	1.1704e + 03
	cond(M_j^{new})	3.6383e + 00	4.5651e + 01	5.0793e + 03	1.9845e + 06
	ϱ^{new}	1.1941e + 00	1.2012e + 00	1.3798e + 00	1.8545e + 00
	cond(Γ_L^{new})	8.0423e + 00	6.0443e + 01	4.8813e + 03	1.1837e + 06
	c_2^{new}/c_1^{new}	3.6516e + 00	3.6500e + 00	3.6500e + 00	3.6500e + 00
B	c_1^{new}	3.4290e − 01	3.4304e − 01	3.4304e − 01	3.4304e − 01
B	c_2^{new}	1.2521e + 00	1.2521e + 00	1.2521e + 00	1.2521e + 00
	$\tilde{c}_2^{new}/\tilde{c}_1^{new}$	4.2543e + 00	3.8336e + 00	4.1049e + 00	4.7450e + 00
b	$\tilde{c}_1^{new}$	8.0199e − 01	7.9896e − 01	7.9959e − 01	7.9952e − 01
=	$\tilde{c}_2^{new}$	3.4119e + 00	3.0629e + 00	3.2822e + 00	3.7937e + 00
1	cond(M_j^{new})	3.4394e + 00	3.1105e + 00	2.8676e + 00	2.8762e + 00
	ϱ^{new}	1.7999e + 00	1.6415e + 00	1.7477e + 00	1.9147e + 00
	cond(Γ_L^{new})	2.8131e + 01	1.5995e + 02	2.4721e + 03	7.3594e + 04
	c_2^{new}/c_1^{new}	6.5163e + 00	6.5150e + 00	6.5150e + 00	6.5150e + 00
B	c_1^{new}	1.8282e − 01	1.8285e − 01	1.8285e − 01	1.8285e − 01
B	c_2^{new}	1.1913e + 00	1.1912e + 00	1.1912e + 00	1.1912e + 00
	$\tilde{c}_2^{new}/\tilde{c}_1^{new}$	7.5633e + 00	6.8110e + 00	7.1891e + 00	7.8499e + 00
b	$\tilde{c}_1^{new}$	8.4307e − 01	8.4023e − 01	8.4109e − 01	8.4085e − 01
=	$\tilde{c}_2^{new}$	6.3764e + 00	5.7228e + 00	6.0467e + 00	6.6006e + 00
2	cond(M_j^{new})	7.1420e + 00	5.5455e + 00	4.7392e + 00	4.7554e + 00
	ϱ^{new}	1.7999e + 00	1.6415e + 00	1.7477e + 00	1.9147e + 00

Table 1.

		$d=3$	$\tilde{d}=3$	$\tilde{d}=5$	$\tilde{d}=7$
N	$\mathrm{cond}(\Gamma_L)$	$1.1944e+03$	$4.3638e+04$	$1.3386e+07$
O	c_2/c_1	$3.3817e+01$	$3.4085e+01$	$3.4085e+01$
	c_1	$3.7026e-01$	$3.6735e-01$	$3.6735e-01$
	c_2	$1.2521e+01$	$1.2521e+01$	$1.2521e+01$
T	$\tilde{c}_2/\tilde{c}_1$	$4.9550e+01$	$3.5748e+01$	$5.5120e+01$
R	$\tilde{c}_1$	$8.5420e-02$	$8.1563e-02$	$8.2273e-02$
A	$\tilde{c}_2$	$4.2326e+00$	$2.9157e+00$	$4.5349e+00$
N	d_2/d_1	$1.6331e+01$	$1.5168e+01$	$1.6809e+01$
S	d_1	$5.6420e-02$	$5.8580e-02$	$7.2344e-02$
F	d_2	$9.2139e-01$	$8.8856e-01$	$1.2160e+00$
O	$\tilde{d}_2/\tilde{d}_1$	$1.8748e+01$	$1.6435e+01$	$2.2899e+01$
R	$\tilde{d}_1$	$1.5789e+00$	$1.2322e+00$	$1.2049e+00$
M	$\tilde{d}_2$	$2.9601e+01$	$2.0252e+01$	$2.7591e+01$
	$\mathrm{cond}(M_j)$	$8.2396e+02$	$8.2396e+02$	$8.3926e+02$
	ϱ	$1.2718e+01$	$9.4964e+00$	$1.1215e+01$
	c_2^{new}/c_1^{new}	$1.6673e+00$	$5.6242e+01$	$2.3651e+03$
	c_1^{new}	$5.9548e-01$	$3.2149e-02$	$1.5930e-03$
S	c_2^{new}	$9.9282e-01$	$1.8081e+00$	$3.7677e+00$
V	$\tilde{c}_2^{new}/\tilde{c}_1^{new}$	$1.8891e+00$	$5.1054e+01$	$1.1585e+03$
D	$\tilde{c}_1^{new}$	$1.0075e+00$	$6.4459e-01$	$5.5096e-01$
	$\tilde{c}_2^{new}$	$1.9032e+00$	$3.2909e+01$	$6.3828e+02$
	$\mathrm{cond}(M_j^{new})$	$1.6431e+01$	$6.2855e+02$	$4.7439e+05$
	ϱ^{new}	$1.9996e+00$	$6.9280e+00$	$7.7156e+00$
	$\mathrm{cond}(\Gamma_L^{new})$	$3.9776e+01$	$9.4989e+02$	$3.1947e+05$
	c_2^{new}/c_1^{new}	$1.9112e+01$	$2.0190e+01$	$2.0190e+01$
B	c_1^{new}	$3.8963e-01$	$3.6882e-01$	$3.6882e-01$
B	c_2^{new}	$7.4465e+00$	$7.4465e+00$	$7.4465e+00$
	$\tilde{c}_2^{new}/\tilde{c}_1^{new}$	$2.8697e+01$	$2.0677e+01$	$2.8880e+01$
b	$\tilde{c}_1^{new}$	$1.4544e-01$	$1.3773e-01$	$1.3897e-01$
=	$\tilde{c}_2^{new}$	$4.1737e+00$	$2.8479e+00$	$4.0135e+00$
1	$\mathrm{cond}(M_j^{new})$	$3.6594e+02$	$3.6640e+02$	$3.6676e+02$
	ϱ^{new}	$4.7280e+00$	$3.3427e+00$	$4.2655e+00$
	$\mathrm{cond}(\Gamma_L^{new})$	$5.6699e+01$	$4.0558e+02$	$2.0585e+04$
	c_2^{new}/c_1^{new}	$8.6997e+00$	$8.8589e+00$	$8.8589e+00$
B	c_1^{new}	$3.7454e-01$	$3.6781e-01$	$3.6781e-01$
B	c_2^{new}	$3.2584e+00$	$3.2584e+00$	$3.2584e+00$
	$\tilde{c}_2^{new}/\tilde{c}_1^{new}$	$1.3470e+01$	$9.3953e+00$	$1.5236e+01$
b	$\tilde{c}_1^{new}$	$3.2236e-01$	$3.1140e-01$	$3.1363e-01$
=	$\tilde{c}_2^{new}$	$4.3421e+00$	$2.9257e+00$	$4.7786e+00$
2	$\mathrm{cond}(M_j^{new})$	$4.7713e+01$	$4.8963e+01$	$4.9679e+01$
	ϱ^{new}	$4.7280e+00$	$3.3427e+00$	$4.2655e+00$

Table 2.

	$d = 4$	$\tilde{d} = 6$	$\tilde{d} = 8$	$\tilde{d} = 10$
	$\mathrm{cond}(\Gamma_L)$	$5.3936e+06$	$4.1889e+08$	$5.3842e+11$
N	c_2/c_1	$3.2086e+02$	$3.2086e+02$	$3.2086e+02$
O	c_1	$1.7203e-01$	$1.7203e-01$	$1.7203e-01$
	c_2	$5.5197e+01$	$5.5197e+01$	$5.5197e+01$
T	$\tilde{c}_2/\tilde{c}_1$	$3.4863e+02$	$3.7829e+02$	$5.5723e+02$
R	$\tilde{c}_1$	$1.8544e-02$	$1.8485e-02$	$1.8368e-02$
A	$\tilde{c}_2$	$6.4652e+00$	$6.9927e+00$	$1.0235e+01$
N	d_2/d_1	$6.9578e+01$	$6.8913e+01$	$7.3206e+01$
S	d_1	$1.1209e-02$	$1.1832e-02$	$1.3706e-02$
F	d_2	$7.7990e-01$	$8.1539e-01$	$1.0034e+00$
O	$\tilde{d}_2/\tilde{d}_1$	$7.1771e+01$	$8.9233e+01$	$1.2030e+02$
R	$\tilde{d}_1$	$1.5343e+00$	$1.3687e+00$	$1.3453e+00$
M	$\tilde{d}_2$	$1.1012e+02$	$1.2213e+02$	$1.6184e+02$
	$\mathrm{cond}(M_j)$	$3.0783e+04$	$3.0785e+04$	$3.1683e+04$
	ϱ	$5.1142e+01$	$5.5315e+01$	$6.5923e+01$
	c_2^{new}/c_1^{new}	$1.1403e+02$	$7.9974e+03$	$3.8262e+05$
	c_1^{new}	$1.3825e-02$	$3.9443e-04$	$1.6616e-05$
S	c_2^{new}	$1.5764e+00$	$3.1544e+00$	$6.3577e+00$
V	$\tilde{c}_2^{new}/\tilde{c}_1^{new}$	$1.2026e+02$	$5.7030e+03$	$1.4805e+05$
D	$\tilde{c}_1^{new}$	$7.7237e-01$	$4.7846e-01$	$4.2143e-01$
	$\tilde{c}_2^{new}$	$9.2884e+01$	$2.7287e+03$	$6.2392e+04$
	$\mathrm{cond}(M_j^{new})$	$6.8133e+03$	$7.1991e+06$	$7.9549e+09$
	ϱ^{new}	$1.3735e+01$	$5.3075e+01$	$5.3066e+01$
	$\mathrm{cond}(\Gamma_L^{new})$	$2.9053e+04$	$2.0258e+06$	$1.3758e+09$
	c_2^{new}/c_1^{new}	$1.3204e+02$	$1.3414e+02$	$1.3414e+02$
B	c_1^{new}	$2.3694e-01$	$2.3323e-01$	$2.3323e-01$
B	c_2^{new}	$3.1286e+01$	$3.1286e+01$	$3.1286e+01$
	$\tilde{c}_2^{new}/\tilde{c}_1^{new}$	$1.5405e+02$	$1.3452e+02$	$2.5570e+02$
b	$\tilde{c}_1^{new}$	$3.2807e-02$	$3.2695e-02$	$3.2468e-02$
$=$	$\tilde{c}_2^{new}$	$5.0539e+00$	$4.3981e+00$	$8.3021e+00$
1	$\mathrm{cond}(M_j^{new})$	$1.2108e+04$	$1.2138e+04$	$1.2339e+04$
	ϱ^{new}	$1.2129e+01$	$1.2882e+01$	$1.5134e+01$
	$\mathrm{cond}(\Gamma_L^{new})$	$5.1602e+03$	$1.4374e+05$	$1.8228e+07$
	c_2^{new}/c_1^{new}	$3.6207e+01$	$3.6192e+01$	$3.6192e+01$
B	c_1^{new}	$2.2077e-01$	$2.2086e-01$	$2.2086e-01$
B	c_2^{new}	$7.9934e+00$	$7.9934e+00$	$7.9934e+00$
	$\tilde{c}_2^{new}/\tilde{c}_1^{new}$	$4.2309e+01$	$4.7187e+01$	$7.9540e+01$
b	$\tilde{c}_1^{new}$	$1.2745e-01$	$1.2704e-01$	$1.2652e-01$
$=$	$\tilde{c}_2^{new}$	$5.3924e+00$	$5.9945e+00$	$1.0063e+01$
2	$\mathrm{cond}(M_j^{new})$	$5.0195e+02$	$5.0688e+02$	$5.3032e+02$
	ϱ^{new}	$1.2129e+01$	$1.2882e+01$	$1.5135e+01$

Table 3.

Remark 6. *Suppose that $\mathbf{C}_j, \tilde{\mathbf{C}}_j$ are any matrices of the form (3.2.3) satisfying (3.2.5), i.e., the corresponding new bases*

$$\Phi_j^{\text{new}} = \mathbf{C}_j \Phi_j, \quad \tilde{\Phi}_j^{\text{new}} = \tilde{\mathbf{C}}_j \tilde{\Phi}_j' \tag{4.6}$$

are biorthogonal. Then the construction (3.3.8) leaves the wavelet bases $\Psi_j, \tilde{\Psi}_j$ unchanged.

Proof: To this end, recall from [18] that the initial stable completion $\check{\mathbf{M}}_{j,1}$ transforms under the change (4.6) into

$$\check{\mathbf{M}}_{j,1}^{\text{new}} = \mathbf{C}_{j+1}^{-T} \check{\mathbf{M}}_{j,1}, \tag{4.7}$$

while

$$\check{\mathbf{G}}_j^{\text{new}} = \begin{pmatrix} \mathbf{C}_j^{-T} \check{\mathbf{G}}_{j,0} \mathbf{C}_{j+1}^T \\ \check{\mathbf{G}}_{j,1} \mathbf{C}_{j+1}^T \end{pmatrix}. \tag{4.8}$$

Now the new wavelets Ψ_j^{new} are given by

$$(\Psi_j^{\text{new}})^T = (\Phi_{j+1}^{\text{new}})^T \mathbf{M}_{j,1}^{\text{new}}, \tag{4.9}$$

where, by (3.3.8),

$$\mathbf{M}_{j,1}^{\text{new}} = (\mathbf{I} - \mathbf{M}_{j,0}^{\text{new}} (\tilde{\mathbf{M}}_{j,0}^{\text{new}})^T) \check{\mathbf{M}}_{j,1}^{\text{new}}.$$

Taking Remark 5 and (4.7) into account yields

$$\begin{aligned}
\mathbf{M}_{j,1}^{\text{new}} &= \mathbf{C}_{j+1}^{-T} (\mathbf{I} - \mathbf{M}_{j,0} \mathbf{C}_j^T \tilde{\mathbf{C}}_j (\tilde{\mathbf{M}}_{j,0}')^T \tilde{\mathbf{C}}_{j+1}^{-1} \mathbf{C}_{j+1}^{-T}) \check{\mathbf{M}}_{j,1} \\
&= \mathbf{C}_{j+1}^{-T} (\mathbf{I} - \mathbf{M}_{j,0} (\Gamma_{j+1} \tilde{\mathbf{M}}_{j,0}' \Gamma_j^{-1})^T) \check{\mathbf{M}}_{j,1} \\
&= \mathbf{C}_{j+1}^{-T} (\mathbf{I} - \mathbf{M}_{j,0} (\tilde{\mathbf{M}}_{j,0})^T) \check{\mathbf{M}}_{j,1} = \mathbf{C}_{j+1}^{-T} \mathbf{M}_{j,1},
\end{aligned}$$

where we have used (3.2.5), (3.2.12) and (3.3.8). Thus, by (4.9), we obtain

$$(\Psi_j^{\text{new}})^T = (\Phi_{j+1}^{\text{new}})^T \mathbf{M}_{j,1}^{\text{new}} = \Phi_{j+1}^T \mathbf{C}_{j+1}^T \mathbf{C}_{j+1}^{-T} \mathbf{M}_{j,1} = \Psi_j^T. \tag{4.10}$$

Similarly, by (3.3.8), (4.6) and (4.8),

$$\begin{aligned}
(\tilde{\Psi}_j^{\text{new}})^T &= (\tilde{\Phi}_{j+1}^{\text{new}})^T \tilde{\mathbf{M}}_{j,1}^{\text{new}} = (\tilde{\Phi}_{j+1}')^T \tilde{\mathbf{C}}_{j+1}^T \mathbf{C}_{j+1} \check{\mathbf{G}}_{j,1}^T \\
&= (\tilde{\Phi}_{j+1}')^T \Gamma_{j+1}^{-1} \check{\mathbf{G}}_{j,1}^T = \tilde{\Phi}_{j+1}^T \tilde{\mathbf{M}}_{j,1} = \tilde{\Psi}_j^T,
\end{aligned}$$

where we have used (3.2.5) and (3.2.10). This confirms the above claim. ∎

We will explore next several strategies for determining appropriate matrices $\mathbf{C}_j, \tilde{\mathbf{C}}_j$ of the form (3.2.3) (but different from (3.2.7)) such that the new bases $\Phi_j^{\text{new}} = \mathbf{C}_j \Phi_j$ and $\tilde{\Phi}_j^{\text{new}} = \tilde{\mathbf{C}}_j \Phi_j'$ are biorthogonal (3.2.2) and have more favorable properties in the above sense. In order to modify also the wavelet bases we would have to employ, on account of Remark 6, nontrivial matrices $\mathbf{K}_j$ in (3.3.8). Since we will dispense with this option here, the Riesz bounds for the wavelet bases will remain unchanged, and thus will not be commented on any longer.

The superscript $^{\text{new}}$ in the quantities $\mathbf{R}_j^{\text{new}}$, c_1^{new}, c_2^{new}, d_1^{new}, d_2^{new} and ϱ^{new} will always indicate the new values resulting from the respective change of bases.

4.1. Singular Value Decomposition

Recall from (3.2.2), (3.2.5) that biorthogonalization essentially requires to determine blocks $\mathbf{C}_L, \check{\mathbf{C}}_L$ such that

$$\mathbf{C}_L \mathbf{\Gamma}_L \check{\mathbf{C}}_L^T = \mathbf{I}. \tag{4.1.1}$$

Our first approach primarily aims at avoiding the numerical problems related to the bad condition of $\mathbf{\Gamma}_L$. The idea is to equidistribute the bad condition of $\mathbf{\Gamma}_L$ to the matrices $\mathbf{C}_L, \check{\mathbf{C}}_L$ as follows. Instead of inverting $\mathbf{\Gamma}_L$ one performs a (more stable) singular value decomposition

$$\mathbf{\Gamma}_L = \mathbf{U}\mathbf{\Sigma}\mathbf{V}^T, \tag{4.1.2}$$

where $\mathbf{\Sigma}$ is diagonal and $\mathbf{U}, \mathbf{V}$ are orthogonal matrices. The choice

$$\mathbf{C}_L := \mathbf{\Sigma}^{-1/2}\mathbf{U}^T, \qquad \check{\mathbf{C}}_L := \mathbf{\Sigma}^{-1/2}\mathbf{V}^T \tag{4.1.3}$$

obviously satisfies (4.1.1) yielding $\text{cond}(\mathbf{\Gamma}_L^{\text{new}}) = 1$.

The second block in Tables 1–3 labeled 'SVD' corresponds to this case. Now the inversion of a possibly extremely ill–conditioned matrix has been avoided completely. In addition the data shows that for the minimal choices $\tilde{d} = d$ the condition of the primal and dual generator bases is also improved significantly. However, for larger $\tilde{d}$, i.e., when aiming at a higher number of vanishing moments the Riesz bounds for the bases Φ_j, $\tilde{\Phi}_j$ and the condition numbers of $\mathbf{M}_j$ become quickly unacceptable.

4.2. Bernstein Basis Polynomials

The following alternative approach addresses primarily the improvement of the Riesz bounds for the generator bases. It is well known that the monomial basis gets increasingly ill–conditioned when the degree d increases. In view of (3.1.1), it is therefore conceivable that the boundary functions inherit this property. This suggests to take up the comments at the end of [18] and work from the beginning with a different boundary adaptation. To describe this, suppose $P_r, r = 0, \ldots, d-1$ is any basis of the space Π_d of polynomials of order d. Defining instead of (3.8) the quantities

$$\eta_{\tilde{\varphi},r}(y) := \langle P_r, \tilde{\varphi}(\cdot - y)\rangle_{\mathbf{R}}, \tag{4.2.1}$$

one still obtains by (3.1.1)

$$\sum_{m\in\mathbb{Z}} \eta_{\tilde{\varphi},r}(m)\,\varphi_{[j,m]}(x) = 2^{j/2}P_r(2^j x), \qquad r = 0, \ldots, d-1. \tag{4.2.2}$$

We will discuss only the left end point of $[0,1]$ since the rest follows again by replacing x by $(1-x)$ and reversing the order of basis polynomials. Let us denote by $\mathbf{Z}_L$ the matrix that takes the monomial basis into the new one

$\mathbf{P} = \{P_r : r = 0, \ldots, d-1\}$, i.e., $P_r(x) = \sum_{l=0}^{d-1}(\mathbf{Z}_L)_{r,l}x^l$. Then one obviously has

$$2^{j/2}P_r(2^j x) = 2^{j/2}\sum_{m\in\mathbb{Z}}\left(\sum_{l=0}^{d-1}(\mathbf{Z}_L)_{r,l}\alpha_{\tilde{\varphi},l}(m)\right)\varphi_{[j,m]}(x),$$

so that

$$\eta_{\tilde{\varphi},r}(m) = \sum_{l=0}^{d-1}(\mathbf{Z}_L)_{r,l}\alpha_{\tilde{\varphi},l}(m) \tag{4.2.3}$$

readily yields the new coefficients. Likewise, choosing also some basis $\tilde{\mathbf{P}}$ for $\Pi_{\tilde{d}}$ with a corresponding transformation $\tilde{\mathbf{Z}}_L$, we obtain as modified boundary functions

$$\Phi_j^{L,\eta} = \mathbf{Z}_L\Phi_j^L, \quad \tilde{\Phi}_j^{L,\tilde{\eta}} = \tilde{\mathbf{Z}}_L\tilde{\Phi}_j^L.$$

Here and in the following we will always assume that the blocks on the primal side are always extended to match the size of those on the dual side as explained earlier. In principle, we could avoid the initial change of $\tilde{\Phi}_j^L$ to $\tilde{\mathbf{Z}}_L\tilde{\Phi}_j^L$. In fact, for $\mathbf{C}_L = \mathbf{Z}_L$ the matrix $\tilde{\mathbf{C}}_L := (\mathbf{Z}_L\Gamma_L)^{-T}$ would provide the biorthogonalized set $\tilde{\Phi}_j^{\mathrm{new},L} = \tilde{\mathbf{C}}_L\tilde{\Phi}_j^L$. However, when working with $\tilde{\mathbf{Z}}_L\tilde{\Phi}_j^L$, instead of $\mathbf{Z}_L\Gamma_L$ the matrix

$$\Gamma_L^\eta = \mathbf{Z}_L\Gamma_L\tilde{\mathbf{Z}}_L^T \tag{4.2.4}$$

has to be inverted. Although one may hope that the above symmetric transformation will favorably effect the condition of Γ_L^η, in our experiments we did not notice much difference between these two choices so that all tests were made with $\mathbf{C}_L = \mathbf{Z}_L$ and $\tilde{\mathbf{C}}_L = (\mathbf{Z}_L\Gamma_L)^{-T}$.

It remains to choose the bases $\mathbf{P}$ and $\tilde{\mathbf{P}}$ for Π_d and $\Pi_{\tilde{d}}$, respectively. In [29], the monomials x^r were replaced by polynomials $p_r(x) = \sum_{i=0}^r a_{r,i}x^i$ trying to find favorable choices of the coefficients $a_{r,i}$. Here we pursue a more systematic strategy replacing the monomial basis by one which is known to be better conditioned. A natural choice would be to employ orthogonal polynomials. On the other hand, it is well–known that *Bernstein basis polynomials* (also known as *Bézier polynomials*) have better stability properties than the monomial basis [24]. These stability properties, of course, depend on the interval with respect to which they are defined. It is not clear beforehand which interval would have the most favorable effect in the present context. Therefore we will consider next the functions $P_r(x) := B_{r;b}^d(x)$ where

$$B_{r;b}^d(x) := b^{-d+1}\binom{d-1}{r}x^r(b-x)^{d-1-r}, \quad r = 0, \ldots, d-1, \tag{4.2.5}$$

are the Bernstein basis polynomials for Π_d with respect to the interval $[0, b]$. The corresponding transformations $\mathbf{Z}_L$ are lower triangular matrices given by

$$(\mathbf{Z})_{r,l} = \begin{cases} (-1)^{r-l}\binom{d-1}{r}\binom{r}{l}b^{-r}, & r \geq l, \\ 0 & \text{otherwise,} \end{cases} \quad l, r = 0, \ldots, d-1. \tag{4.2.6}$$

The inverse transformation is known to be

$$(\mathbf{Z}^{-1})_{r,l} = \begin{cases} b^l \binom{r}{l} / \binom{d-1}{r}, & r \geq l, \\ 0 & \text{otherwise}, \end{cases} \qquad l, r = 0, \ldots, d-1, \qquad (4.2.7)$$

cf. [24]. The matrices $\tilde{\mathbf{Z}}_L$, $\tilde{\mathbf{Z}}_L^{-1}$ can be defined analogously with d replaced by $\tilde{d}$.

As before we leave the primal sets $\Phi_j^L = \Phi^{L,\eta}$, defined relative to the Bernstein basis as decribed above, fixed, and biorthogonalize the dual sets. The resulting entities are again indexed by the superscript ^{new}. In order to facilitate the comparison of the results to the previous cases, we have displayed in the third part of Tables 1–3 some data where the Bernstein basis transformation was applied relative to the choices $b = 1$ and $b = 2$. In order to show the quite remarkable influence of the parameter b, the results for various combinations of d and $\tilde{d}$ are listed for several choices of b in Tables 4–14. In these tables, the respective most favorable choice of b for the condition numbers of $\mathbf{R}_j^{new}$ and $\mathbf{\Gamma}_L^{new}$ are marked in boldface. Note that the parameter ϱ is unaffected by the different choices of b.

$d = 2, \ \tilde{d} = 2$ Using no transformation, SVD–based transformation and Bernstein basis transformation for different values of b					
	cond($\mathbf{\Gamma}_L$)	c_2/c_1	$\tilde{c}_2/\tilde{c}_1$	cond($\mathbf{M}_j$)	ϱ
NoTr.	$1.6774e+01$	$4.4422e+00$	$5.0473e+00$	$5.3641e+00$	$2.5454e+00$
SVD	$1.0000e+00$	$1.6673e+00$	$1.8891e+00$	$3.6383e+00$	$1.1941e+00$
0.4	$\mathbf{3.9964e+00}$	$3.0928e+00$	$\mathbf{3.4956e+00}$	$4.1684e+00$	$1.7999e+00$
0.7	$4.8656e+00$	$\mathbf{3.0100e+00}$	$3.5034e+00$	$\mathbf{2.8652e+00}$	$1.7999e+00$
1.0	$8.0423e+00$	$3.6516e+00$	$4.2543e+00$	$3.4394e+00$	$1.7999e+00$

Table 4.

$d = 2, \ \tilde{d} = 4$ Using no transformation, SVD–based transformation and Bernstein basis transformation for different values of b					
	cond($\mathbf{\Gamma}_L$)	c_2/c_1	$\tilde{c}_2/\tilde{c}_1$	cond($\mathbf{M}_j$)	ϱ
NoTr.	$7.2772e+02$	$4.4413e+00$	$4.6054e+00$	$4.7432e+00$	$2.5454e+00$
SVD	$1.0000e+00$	$1.1350e+01$	$1.0796e+01$	$4.5651e+01$	$1.2012e+00$
0.5	$1.5131e+02$	$\mathbf{2.8738e+00}$	$\mathbf{3.0364e+00}$	$3.3416e+00$	$1.6415e+00$
0.7	$7.9050e+01$	$3.0061e+00$	$3.1712e+00$	$\mathbf{2.5986e+00}$	$1.6415e+00$
1.0	$\mathbf{6.0443e+01}$	$3.6500e+00$	$3.8336e+00$	$3.1105e+00$	$1.6415e+00$
2.0	$1.5995e+02$	$6.5150e+00$	$6.8110e+00$	$5.5455e+00$	$1.6415e+00$

Table 5.

	cond(Γ_L)	c_2/c_1	$\tilde{c}_2/\tilde{c}_1$	cond(M_j)	ϱ
NoTr.	$1.8741e + 05$	$4.4413e + 00$	$4.8294e + 00$	$4.4225e + 00$	$2.4038e + 00$
SVD	$1.0000e + 00$	$2.2554e + 02$	$1.8861e + 02$	$5.0793e + 03$	$1.3798e + 00$
0.5	$7.4039e + 04$	$\mathbf{2.8736e + 00}$	$3.3902e + 00$	$3.4997e + 00$	$1.7477e + 00$
0.6	$3.3843e + 04$	$2.8856e + 00$	$\mathbf{3.3621e + 00}$	$2.9531e + 00$	$1.7477e + 00$
0.8	$1.0715e + 04$	$3.1880e + 00$	$3.6329e + 00$	$\mathbf{2.5200e + 00}$	$1.7477e + 00$
1.0	$4.8813e + 03$	$3.6500e + 00$	$4.1049e + 00$	$2.8676e + 00$	$1.7477e + 00$
1.6	$\mathbf{2.0975e + 03}$	$5.3218e + 00$	$5.8936e + 00$	$3.9648e + 00$	$1.7477e + 00$
2.0	$2.4721e + 03$	$6.5150e + 00$	$7.1891e + 00$	$4.7392e + 00$	$1.7477e + 00$

Table title above: $d = 2, \ \tilde{d} = 6$ — Using no transformation, SVD–based transformation and Bernstein basis transformation for different values of b

Table 6.

	cond(Γ_L)	c_2/c_1	$\tilde{c}_2/\tilde{c}_1$	cond(M_j)	ϱ
NoTr.	$1.1515e + 08$	$4.4413e + 00$	$5.3946e + 00$	$4.4280e + 00$	$2.5803e + 00$
SVD	$1.0000e + 00$	$6.8118e + 03$	$4.2374e + 03$	$1.9845e + 06$	$1.8545e + 00$
0.5	$7.6865e + 07$	$\mathbf{2.8736e + 00}$	$4.4703e + 00$	$3.8173e + 00$	$1.9147e + 00$
0.7	$9.3902e + 06$	$3.0061e + 00$	$\mathbf{4.2795e + 00}$	$2.9001e + 00$	$1.9147e + 00$
0.8	$4.2318e + 06$	$3.1880e + 00$	$4.3706e + 00$	$\mathbf{2.6746e + 00}$	$1.9147e + 00$
1.0	$1.1837e + 06$	$3.6500e + 00$	$4.7450e + 00$	$2.8762e + 00$	$1.9147e + 00$
2.0	$7.3594e + 04$	$6.5150e + 00$	$7.8499e + 00$	$4.7554e + 00$	$1.9147e + 00$
2.2	$\mathbf{7.0390e + 04}$	$7.1210e + 00$	$8.5445e + 00$	$5.1849e + 00$	$1.9147e + 00$
3.0	$9.2374e + 04$	$9.5762e + 00$	$1.1389e + 01$	$8.0034e + 00$	$1.9147e + 00$

Table title above: $d = 2, \ \tilde{d} = 8$ — Using no transformation, SVD–based transformation and Bernstein basis transformation for different values of b

Table 7.

	cond(Γ_L)	c_2/c_1	$\tilde{c}_2/\tilde{c}_1$	cond(M_j)	ϱ
NoTr.	$1.1944e + 03$	$3.3817e + 01$	$4.9550e + 01$	$8.2396e + 02$	$1.2718e + 01$
SVD	$1.0000e + 00$	$1.6673e + 00$	$1.8891e + 00$	$1.6431e + 01$	$1.9996e + 00$
1.0	$3.9776e + 01$	$1.9112e + 01$	$2.8697e + 01$	$3.6594e + 02$	$4.7280e + 00$
1.2	$\mathbf{3.5235e + 01}$	$1.4865e + 01$	$2.2500e + 01$	$2.0266e + 02$	$4.7280e + 00$
2.0	$5.6699e + 01$	$\mathbf{8.6997e + 00}$	$1.3470e + 01$	$4.7713e + 01$	$4.7280e + 00$
3.0	$1.3161e + 02$	$1.3047e + 01$	$2.0005e + 01$	$2.2125e + 01$	$4.7280e + 00$
3.6	$2.1907e + 02$	$1.7166e + 01$	$2.6445e + 01$	$\mathbf{2.0191e + 01}$	$4.7280e + 00$
4.0	$3.0370e + 02$	$2.0412e + 01$	$3.1534e + 01$	$2.2290e + 01$	$4.7280e + 00$

Table title above: $d = 3, \ \tilde{d} = 3$ — Using no transformation, SVD–based transformation and Bernstein basis transformation for different values of b

Table 8.

$d = 3, \quad \tilde{d} = 5$ Using no transformation, SVD–based transformation and Bernstein basis transformation for different values of b					
	cond(Γ_L)	c_2/c_1	$\tilde{c}_2/\tilde{c}_1$	cond(M_j)	ϱ
NoTr.	$4.3638e + 04$	$3.4085e + 01$	$3.5748e + 01$	$8.2396e + 02$	$9.4964e + 00$
SVD	$1.0000e + 00$	$5.6242e + 01$	$5.1054e + 01$	$6.2855e + 02$	$6.9280e + 00$
1.0	$9.4989e + 02$	$2.0190e + 01$	$2.0677e + 01$	$3.6640e + 02$	$3.3427e + 00$
1.7	$\mathbf{3.6213e + 02}$	$1.0375e + 01$	$1.0713e + 01$	$7.3457e + 01$	$3.3427e + 00$
2.0	$4.0558e + 02$	$8.8589e + 00$	$\mathbf{9.3953e + 00}$	$4.8963e + 01$	$3.3427e + 00$
2.1	$4.3173e + 02$	$\mathbf{8.7474e + 00}$	$9.6467e + 00$	$4.3879e + 01$	$3.3427e + 00$
3.0	$9.2645e + 02$	$1.3044e + 01$	$1.4436e + 01$	$2.5398e + 01$	$3.3427e + 00$
3.7	$1.7714e + 03$	$1.7938e + 01$	$1.9892e + 01$	$\mathbf{2.3535e + 01}$	$3.3427e + 00$
4.0	$2.3241e + 03$	$2.0410e + 01$	$2.2648e + 01$	$2.3791e + 01$	$3.3427e + 00$

Table 9.

$d = 3, \quad \tilde{d} = 7$ Using no transformation, SVD–based transformation and Bernstein basis transformation for different values of b					
	cond(Γ_L)	c_2/c_1	$\tilde{c}_2/\tilde{c}_1$	cond(M_j)	ϱ
NoTr.	$1.3386e + 07$	$3.4085e + 01$	$5.5120e + 01$	$8.3926e + 02$	$1.1215e + 01$
SVD	$1.0000e + 00$	$2.3651e + 03$	$1.1585e + 03$	$4.7439e + 05$	$7.7156e + 00$
1.0	$3.1947e + 05$	$2.0190e + 01$	$2.8880e + 01$	$3.6676e + 02$	$4.2655e + 00$
2.0	$2.0585e + 04$	$8.8589e + 00$	$1.5236e + 01$	$4.9679e + 01$	$4.2655e + 00$
2.1	$1.9148e + 04$	$\mathbf{8.7474e + 00}$	$\mathbf{1.5197e + 01}$	$4.4684e + 01$	$4.2655e + 00$
2.5	$\mathbf{1.7321e + 04}$	$1.0326e + 01$	$1.6203e + 01$	$3.2779e + 01$	$4.2655e + 00$
3.0	$1.9540e + 04$	$1.3044e + 01$	$1.9284e + 01$	$2.7239e + 01$	$4.2655e + 00$
3.5	$2.5171e + 04$	$1.6414e + 01$	$2.3709e + 01$	$\mathbf{2.5962e + 01}$	$4.2655e + 00$
4.0	$3.4692e + 04$	$2.0410e + 01$	$2.9190e + 01$	$2.6544e + 01$	$4.2655e + 00$

Table 10.

$d = 4, \quad \tilde{d} = 6$ Using no transformation, SVD–based transformation and Bernstein basis transformation for different values of b					
	cond(Γ_L)	c_2/c_1	$\tilde{c}_2/\tilde{c}_1$	cond(M_j)	ϱ
NoTr.	$5.3936e + 06$	$3.2086e + 02$	$3.4863e + 02$	$3.0783e + 04$	$5.1142e + 01$
SVD	$1.0000e + 00$	$1.1403e + 02$	$1.2026e + 02$	$6.8133e + 03$	$1.3735e + 01$
1.0	$2.9053e + 04$	$1.3204e + 02$	$1.5405e + 02$	$1.2108e + 04$	$1.2129e + 01$
1.8	$\mathbf{4.7779e + 03}$	$4.0413e + 01$	$4.7383e + 01$	$7.7721e + 02$	$1.2129e + 01$
2.0	$5.1602e + 03$	$\mathbf{3.6207e + 01}$	$4.2309e + 01$	$5.0195e + 02$	$1.2129e + 01$
3.0	$1.4593e + 04$	$6.2076e + 01$	$7.1896e + 01$	$1.1328e + 02$	$1.2129e + 01$
3.6	$2.9962e + 04$	$8.5930e + 01$	$9.9810e + 01$	$\mathbf{7.7863e + 01}$	$1.2129e + 01$
4.0	$4.7815e + 04$	$1.0576e + 02$	$1.2306e + 02$	$8.3699e + 01$	$1.2129e + 01$

Table 11.

	cond(Γ_L)	c_2/c_1	$\tilde{c}_2/\tilde{c}_1$	cond($\mathbf{M}_j$)	ϱ
	\multicolumn{5}{c}{$d=4,\ \tilde{d}=8$}				

Full header:

\multicolumn{6}{c}{$d=4,\ \tilde{d}=8$ Using no transformation, SVD–based transformation and Bernstein basis transformation for different values of b}
	cond(Γ_L)	c_2/c_1	$\tilde{c}_2/\tilde{c}_1$	cond($\mathbf{M}_j$)	ϱ
---	---	---	---	---	---
NoTr.	$4.1889e+08$	$3.2086e+02$	$3.7829e+02$	$3.0785e+04$	$5.5315e+01$
SVD	$1.0000e+00$	$7.9974e+03$	$5.7030e+03$	$7.1991e+06$	$5.3075e+01$
1.0	$2.0258e+06$	$1.3414e+02$	$1.3452e+02$	$1.2138e+04$	$1.2882e+01$
1.8	$1.6771e+05$	$4.0993e+01$	$\mathbf{4.6009e+01}$	$7.8265e+02$	$1.2882e+01$
2.0	$1.4374e+05$	$\mathbf{3.6192e+01}$	$4.7187e+01$	$5.0688e+02$	$1.2882e+01$
2.2	$\mathbf{1.3822e+05}$	$3.9768e+01$	$5.1245e+01$	$3.4835e+02$	$1.2882e+01$
3.0	$2.2134e+05$	$6.2076e+01$	$7.9070e+01$	$1.1842e+02$	$1.2882e+01$
4.0	$6.2401e+05$	$1.0576e+02$	$1.3511e+02$	$6.5476e+01$	$1.2882e+01$
4.1	$6.9575e+05$	$1.1127e+02$	$1.4220e+02$	$\mathbf{6.5473e+01}$	$1.2882e+01$

Table 12.

$d=4,\ \tilde{d}=10$ Using no transformation, SVD–based transformation and Bernstein basis transformation for different values of b
	cond(Γ_L)	c_2/c_1	$\tilde{c}_2/\tilde{c}_1$	cond($\mathbf{M}_j$)	ϱ
---	---	---	---	---	---
NoTr.	$5.3842e+11$	$3.2086e+02$	$5.5723e+02$	$3.1683e+04$	$6.5923e+01$
SVD	$1.0000e+00$	$3.8262e+05$	$1.4805e+05$	$7.9549e+09$	$5.3066e+01$
1.0	$1.3758e+09$	$1.3414e+02$	$2.5575e+02$	$1.2339e+04$	$1.5134e+01$
2.0	$1.8228e+07$	$\mathbf{3.6192e+01}$	$7.9535e+01$	$5.3032e+02$	$1.5134e+01$
2.2	$1.2880e+07$	$3.9768e+01$	$\mathbf{7.7667e+01}$	$3.6866e+02$	$1.5135e+01$
3.0	$\mathbf{8.1173e+06}$	$6.2076e+01$	$1.0200e+02$	$1.3781e+02$	$1.5134e+01$
4.0	$1.2753e+07$	$1.0576e+02$	$1.6981e+02$	$8.6679e+01$	$1.5134e+01$
4.4	$1.7456e+07$	$1.2922e+02$	$2.0728e+02$	$\mathbf{8.3882e+01}$	$1.5135e+01$

Table 13.

$d=5,\ \tilde{d}=7$ Using no transformation, SVD–based transformation and Bernstein basis transformation for different values of b
	cond(Γ_L)	c_2/c_1	$\tilde{c}_2/\tilde{c}_1$	cond($\mathbf{M}_j$)	ϱ
---	---	---	---	---	---
NoTr.	$1.0539e+10$	$1.0766e+04$	$1.0678e+04$	$4.1464e+07$	$1.7658e+02$
SVD	$1.0000e+00$	$3.3800e+02$	$1.1018e+03$	$4.2393e+04$	$1.0276e+00$
2.0	$3.9536e+05$	$6.9462e+02$	$6.8983e+02$	$1.4737e+05$	$6.9246e+01$
2.7	$\mathbf{2.2764e+05}$	$3.0269e+02$	$3.0098e+02$	$2.3004e+04$	$6.9246e+01$
3.0	$2.3930e+05$	$2.3173e+02$	$2.3034e+02$	$1.2601e+04$	$6.9246e+01$
3.1	$2.4792e+05$	$\mathbf{2.2210e+02}$	$2.1250e+02$	$1.0527e+04$	$6.9246e+01$
3.2	$2.5869e+05$	$2.2768e+02$	$\mathbf{1.9678e+02}$	$8.8830e+03$	$6.9246e+01$
4.0	$4.2676e+05$	$3.0494e+02$	$2.5160e+02$	$3.2708e+03$	$6.9246e+01$
5.7	$1.7141e+06$	$5.9374e+02$	$4.8053e+02$	$\mathbf{2.0130e+03}$	$6.9246e+01$
6.0	$2.2060e+06$	$6.6513e+02$	$5.3756e+02$	$2.0211e+03$	$6.9246e+01$

Table 14.

4.3. Conclusion

The results from Tables 4–14 confirm that throughout the full range of choices for $d, \tilde{d}$, a transformation of the standard generator bases $\Phi_j, \tilde{\Phi}_j$ using the Bernstein basis transformation for a well–chosen b improves the condition of the primal and dual generator bases, of the transformation $\mathbf{M}_j$ as well as of the matrix $\boldsymbol{\Gamma}_L$ significantly. This effect increases with d but is rather insensitive with respect to $\tilde{d}$. Only for $d = \tilde{d} = 2$ the SVD technique gives slightly better results. For instance, for $d = 4, \tilde{d} = 10$ the condition of $\boldsymbol{\Gamma}_L$ is improved through the Bernstein–Bézier transformation by a factor 10^5 while cond($\mathbf{M}_j$) is reduced by approximately 10^3. Although the respective optimal values of the investigated quantities vary with b, the data reveals that an appropriate compromise (e.g. chosing $b = 3.0$ for $d = 4, \tilde{d} = 10$) still yields a significant improvement over the standard setting. The detailed account of our experiments documented in Tables 4–14 shows which combination of parameters is best for a given priority.

§5. Plots

We conclude with illustrating the above findings by a series of plots comparing the initial and Bernstein basis stabilized bases at the left boundary (recall the symmetry properties of the bases). As an example we choose $d = 4, \tilde{d} = 8$ for which the various effects caused by the Bernstein basis transformation are more visible than in the lower order cases. The functions were stabilized relative to $b = 2.0$ for which, according to Table 12, the condition of Φ_j and $\tilde{\Phi}_j$ yields a good compromise. All functions are plotted relative to level $j = j_0 = 6$. In Figure 3 we show all the four primal generators which are modified at the boundary before and after the transformation in addition to the first interior one. Figure 4 shows a selection of the modified dual generators, namely, $\tilde{\varphi}^L_{j,\ell-d+r}$ for $r = 0, 1, 2, 7$ and the first interior one. The difference to the other boundary functions not displayed here was not visible. Finally, in Figure 5 we have plotted the wavelets and dual wavelets at the boundary which, as was mentioned in Remark 6, are not affected by the Bernstein basis transformation. Also we only display a selection of them including the first interior one. One should note that the sup–norm of the boundary adapted basis functions is reduced significantly by the stabilizing transformations.
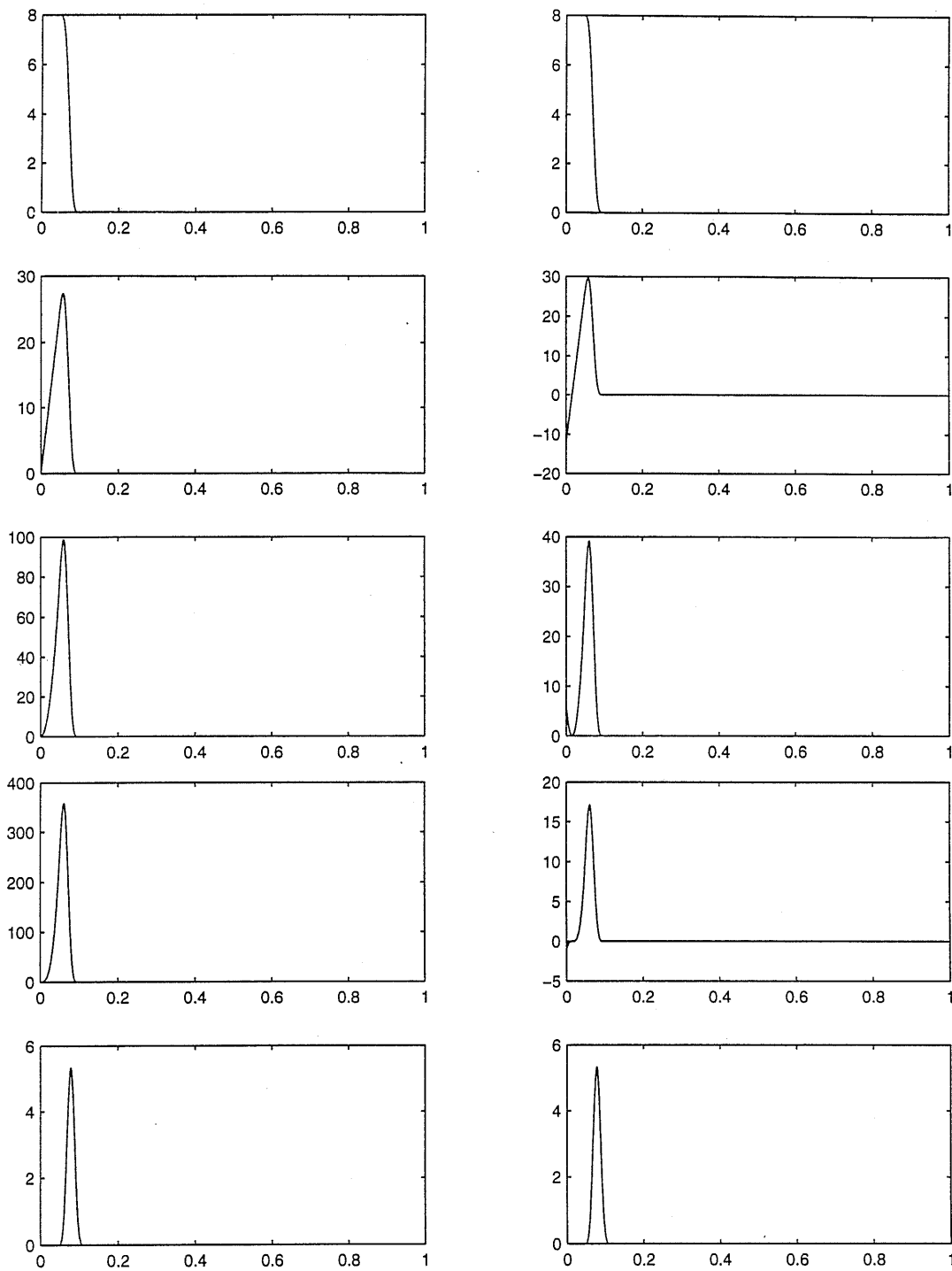
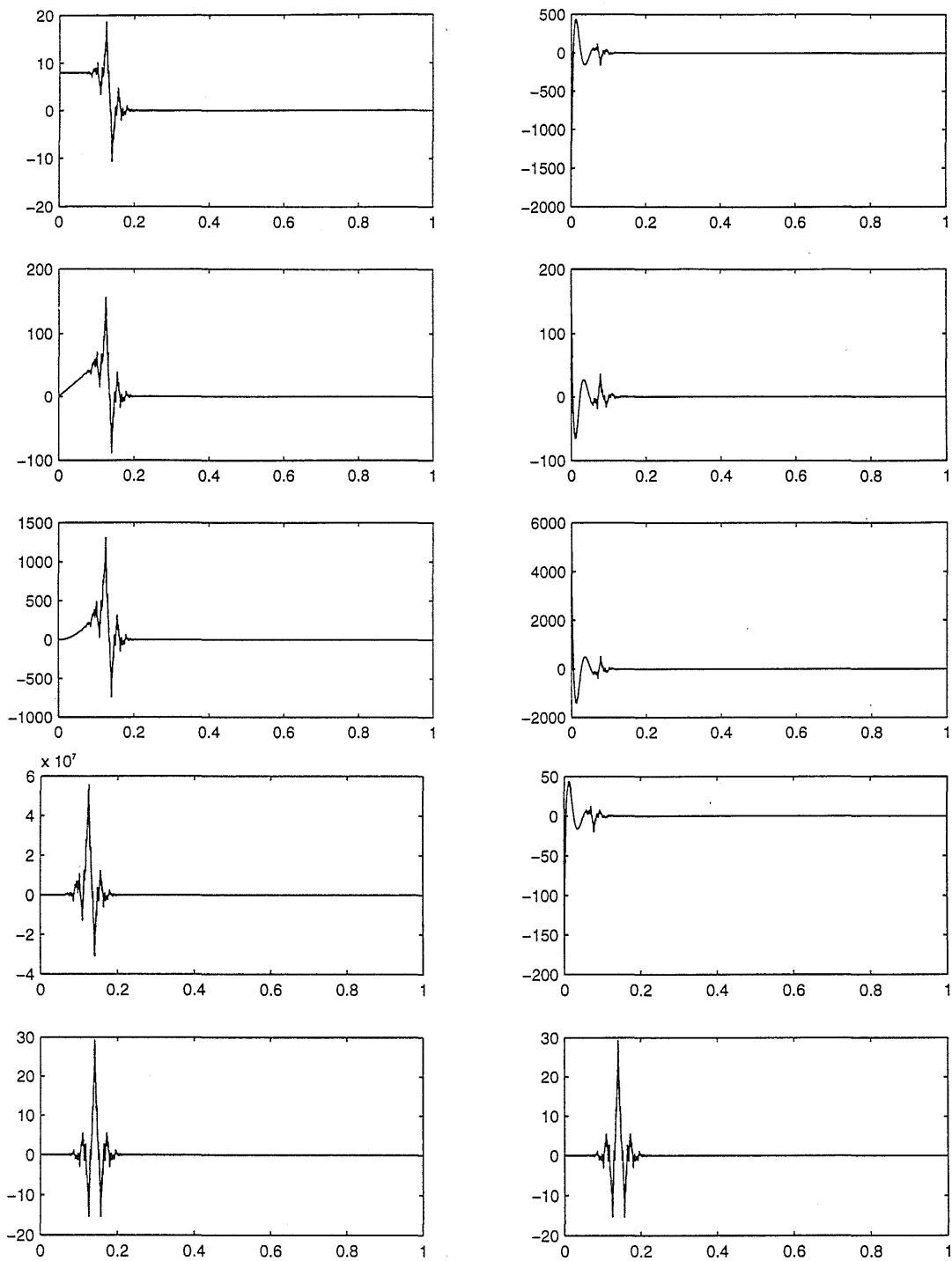**Fig. 3.** Primal generators: Φ_j (left column) and Φ_j^{new} (right column).

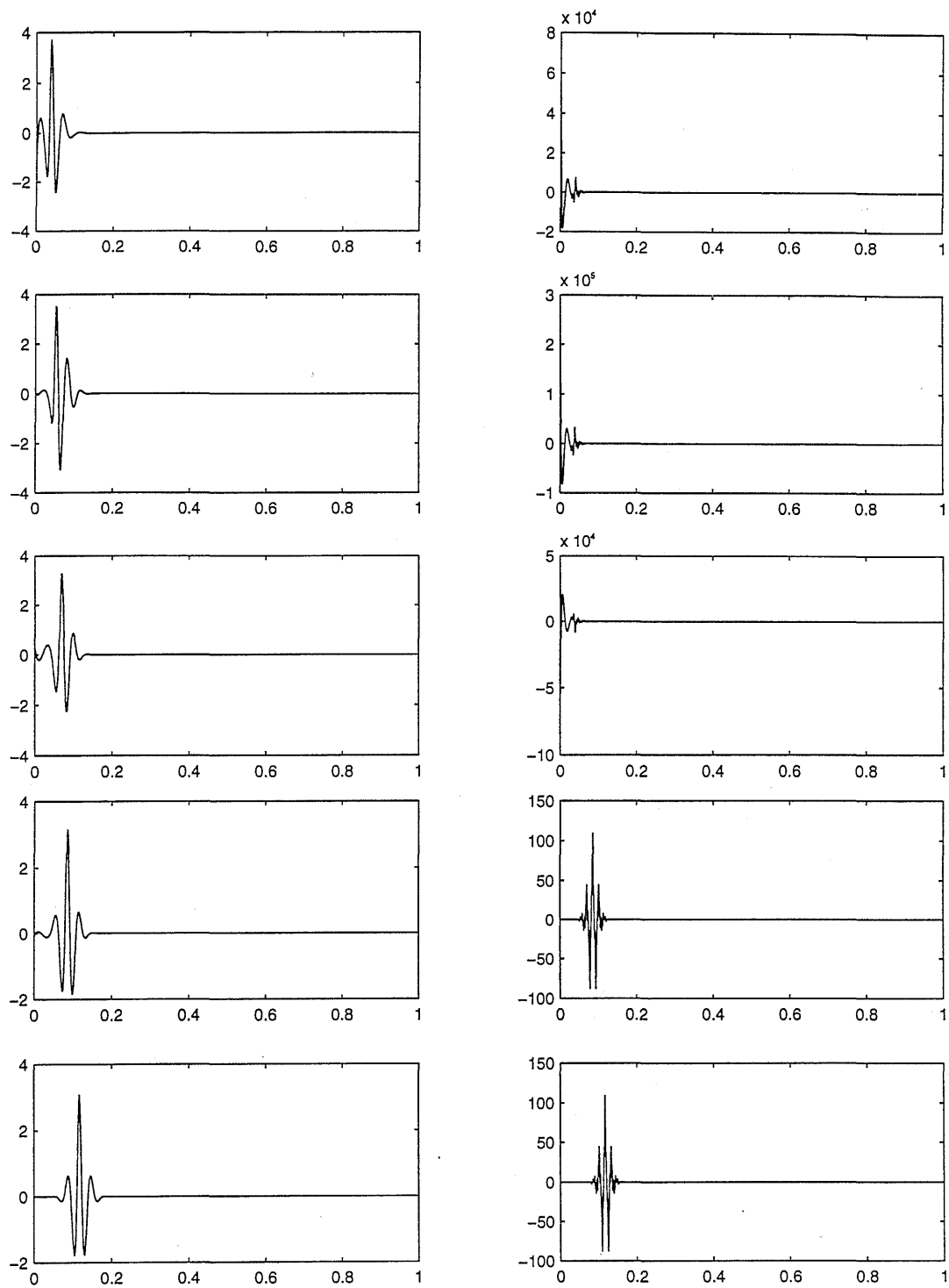**Fig. 4.** Dual generators: $\tilde{\Phi}_j$ (left column) and $\tilde{\Phi}_j^{new}$ (right column).

Fig. 5. Wavelets: Ψ_j (left column) and $\tilde{\Psi}_j$ (right column).

References

1. R.A. Adams, *Sobolev Spaces*, Academic Press, 1978.
2. B. Alpert, A class of bases in L_2 for sparse representation of integral operators, SIAM J. Math. Anal. **24**, 1993, 159–184.
3. L. Andersson, N. Hall, B. Jawerth and G. Peters, Wavelets on closed subsets of the real line, in: *Topics in the Theory and Applications of Wavelets*, L.L. Schumaker and G. Webb (eds.), Academic Press, Boston, 1994, 1–61.
4. A. Averbuch, G. Beylkin, R. Coifman and M. Israeli, Multiscale inversion of elliptic operators, in: *Signal and Image Representation in Combined Spaces*, J. Zeevi and R. Coifman (eds.), Academic Press, Boston, 1995, 1–16.
5. I. Babuška, The finite element method with Lagrange multipliers, Numer. Math. **20**, 1973, 179–192.
6. C. Canuto, A. Tabacco and K. Urban, WEM — The wavelet element method, in preparation.
7. J.M. Carnicer, W. Dahmen and J.M. Peña, Local decomposition of refinable spaces, Appl. Comp. Harm. Anal. **3**, 1996, 127–153.
8. C.K. Chui, *An Introduction to Wavelets*, Academic Press, 1992.
9. C.K. Chui and E. Quak, Wavelets on a bounded interval, in: *Numerical Methods of Approximation Theory*, D. Braess and L.L. Schumaker (eds.), Birkhäuser, 1992, 1–24.
10. Z. Ciesielski and J. Figiel, Spline bases in classical function spaces on compact C^∞ manifolds, part I&II, Studia Math., **76**, 1983, 1–58, 95–136.
11. A. Cohen and I. Daubechies, Non–separable bidimensional wavelet bases, Revista Mat. Iberoamericana **9**, 1993, 51–137.
12. A. Cohen, I. Daubechies and J.-C. Feauveau, Biorthogonal bases of compactly supported wavelets, Comm. Pure and Appl. Math. **45**, 1992, 485–560.
13. A. Cohen, I. Daubechies and P. Vial, Wavelets on the interval and fast wavelet transforms, Appl. Comp. Harm. Anal. **1**, 1993, 54–81.
14. A. Cohen, W. Dahmen and R.A. DeVore, Multiscale decompositions on bounded domains, RWTH Aachen, IGPM preprint No. 113, 1995.
15. S. Dahlke, W. Dahmen, R. Hochmuth and R. Schneider, Stable multiscale bases and local error estimation for elliptic problems, RWTH Aachen, IGPM preprint No. 124, 1996, to appear in Applied Numerical Mathematics, 1997.
16. W. Dahmen, Wavelet and multiscale methods for operator equations, to appear in Acta Numerica, 1997.
17. W. Dahmen, A. Kunoth and K. Urban, A wavelet–Galerkin method for the Stokes problem, Computing **56**, 1996, 259–302.
18. W. Dahmen, A. Kunoth and K. Urban, Biorthogonal spline–wavelets on the interval — Stability and moment conditions, RWTH Aachen, IGPM preprint No. 129, 1996.

19. W. Dahmen, S. Prößdorf, R. Schneider, Multiscale methods for pseudo-differential equations on smooth manifolds, in: *Proceedings of the International Conference on Wavelets: Theory, Algorithms, and Applications*, C.K. Chui, L. Montefusco, L. Puccio (eds.), Academic Press, 1994, 385–424.

20. W. Dahmen and R. Schneider, Composite wavelet bases for operator equations, RWTH Aachen, IGPM preprint No. 133, 1996.

21. W. Dahmen and R. Schneider, Wavelets on manifolds I: Construction and domain decomposition, in preparation.

22. I. Daubechies, *Ten Lectures on Wavelets*, CBMS–NSF Regional Conference Series in Applied Mathematics **61**, 1992.

23. G.C. Donovan, J.S. Geronimo and D.P. Hardin, Orthogonal polynomials and the construction of piecewise polynomial smooth wavelets, preprint 1997.

24. R.T. Farouki and C.A. Neff, On the numerical condition of Bernstein-Bézier subdivision processes, Math. Comp. **55**, 1990, 637–647.

25. R. Glowinski, T.W. Pan, R.O. Wells and X. Zhou, Wavelet and finite element solutions for the Neumann problem using fictitious domains, J. Comput. Phys. **126**, 1996, 40–51.

26. A. Jouini and P.G. Lemarié–Rieusset, Ondelettes sur un ouvert borné du plan, Université de Paris–Sud, preprint 92–46, 1992.

27. A. Kunoth, Multilevel preconditioning — Appending boundary conditions by Lagrange multipliers, Advances in Computational Mathematics 4, 1995, 145–170.

28. P.G. Lemarié–Rieusset, Analyses multirésolutions non orthogonales, commutation entre projecteurs et derivation et ondelettes vecteurs à divergence nulle, Revista Mat. Iberoamericana 8, 1992, 221–236.

29. R. Masson, Biorthogonal spline wavelets on the interval for the resolution of boundary problems, Mathematical Models in Applied Sciences 6, 1996, 749–791.

30. Y. Meyer, *Ondelettes et Opérateurs I*, Hermann, Paris 1990.

31. G. Plonka, Approximation order provided by refinable function vectors, to appear in Constr. Approx., 1997.

32. K. Urban, On divergence–free wavelets, Advances in Computational Mathematics 4, 1995, 51–82.

33. K. Urban, A wavelet–Galerkin algorithm for the driven–cavity–Stokes-problem in two space dimensions, in: *Numerical Modelling in Continuum Mechanics*, M. Feistauer, R. Rannacher, K. Kozel (eds.), Prague, 1995, 278–289.

Wolfgang Dahmen
Institut für Geometrie und Praktische Mathematik
RWTH Aachen, 52056 Aachen, GERMANY
dahmen@igpm.rwth-aachen.de
http://www.igpm.rwth-aachen.de/~dahmen

Angela Kunoth
Weierstrass–Institut für Angewandte Analysis und Stochastik (WIAS)
Mohrenstr. 39
10117 Berlin, GERMANY
kunoth@wias-berlin.de
http://www.igpm.rwth-aachen.de/~kunoth

Karsten Urban
Institut für Geometrie und Praktische Mathematik
RWTH Aachen
52056 Aachen, GERMANY
urban@igpm.rwth-aachen.de
http://www.igpm.rwth-aachen.de/~urban

Recent publications of the
Weierstraß–Institut für Angewandte Analysis und Stochastik

Preprints 1996

292. Peter E. Kloeden, Eckhard Platen, Henri Schurz, Michael Sørensen: On effects of discretization on estimators of drift parameters for diffusion processes.

293. Erlend Arge, Angela Kunoth: An efficient ADI–solver for scattered data problems with global smoothing.

294. Alfred Liemant, Ludwig Brehmer: A mean field approximation for hopping transport in disordered materials.

295. Michael H. Neumann: Strong approximation of density estimators from weakly dependent observations by density estimators from independent observations.

296. Lida V. Gilyova, Vladimir V. Shaidurov: A cascadic multigrid algorithm in the finite element method for the plane elasticity problem.

297. Oleg Lepski, Arkadi Nemirovski, Vladimir Spokoiny: On estimation of non–smooth functionals.

298. Luis Barreira, Yakov Pesin, Jörg Schmeling: On a general concept of multifractality: Multifractal spectra for dimensions, entropies, and Lyapunov exponents. Multifractal rigidity.

299. Luis Barreira, Jörg Schmeling: Any set of irregular points has full Hausdorff dimension and full topological entropy.

300. Jörg Schmeling: On the completeness of multifractal spectra.

301. Yury Kutoyants, Vladimir Spokoiny: Optimal choice of observation window for Poisson observations.

302. Sanjeeva Balasuriya, Christopher K.R.T. Jones, Björn Sandstede: Viscous perturbations of vorticity conserving flows and separatrix splitting.

303. Pascal Chossat, Frédéric Guyard, Reiner Lauterbach: Generalized heteroclinic cycles in spherically invariant systems and their perturbations.

304. Klaus R. Schneider: Decomposition and diagonalization in solving large systems.

305. Klaus Fleischmann, Achim Klenke: Convergence to a non–trivial equilibrium for two–dimensional catalytic super–Brownian motion.

306. Klaus Fleischmann, Vladimir A. Vatutin: Reduced subcritical Galton–Watson processes in a random environment.

Preprints 1997

307. Andreas Rathsfeld: On the stability of piecewise linear wavelet collocation and the solution of the double layer equation over polygonal curves.

308. Georg Hebermehl, Rainer Schlundt, Horst Zscheile, Wolfgang Heinrich: Eigen mode solver for microwave transmission lines.

309. Georg Hebermehl, Rainer Schlundt, Horst Zscheile, Wolfgang Heinrich: Improved numerical solutions for the simulation of microwave circuits.

310. Krzysztof Wilmański: The thermodynamical model of compressible porous materials with the balance equation of porosity.

311. Hans Günter Bothe: Strange attractors with topologically simple basins.

312. Krzysztof Wilmański: On the acoustic waves in two–component linear poroelastic materials.

313. Peter Mathé: Relaxation of product Markov chains on product spaces.

314. Vladimir Spokoiny: Testing a linear hypothesis using Haar transform.

315. Dietmar Hömberg, Jan Sokołowski: Optimal control of laser hardening.

316. Georg Hebermehl, Rainer Schlundt, Horst Zscheile, Wolfgang Heinrich: Numerical solutions for the simulation of monolithic microwave integrated circuits.

317. Donald A. Dawson, Klaus Fleischmann, Guillaume Leduc: Continuous dependence of a class of superprocesses on branching parameters, and applications.

318. Peter Mathé: Asymptotically optimal weighted numerical integration.

319. Guillaume Leduc: Martingale problem for (ξ, Φ, k)–superprocesses.

320. Sergej Rjasanow, Thomas Schreiber, Wolfgang Wagner: Reduction of the number of particles in the stochastic weighted particle method for the Boltzmann equation.